AUS DER KLINIK FÜR AUGENHEILKUNDE DER UNIVERSITÄT ZU LÜBECK

DIREKTOR: PROF. DR. SALVATORE GRISANTI

The effects of Rho-kinase inhibitor H-1152P, the dyes acid violet-17 and indocyanine green on retinal function in the electrophysiological model of the isolated and perfused vertebrate retina

Inauguraldissertation zur

Erlangung der Doktorwürde

der Universität zur Lübeck
- aus der Sektion Medizin -

Vorgelegt von

Aizhan Alt

aus Almaty

Kasachstan

Lübeck 2015

1. Berichterstatter: Priv.-Doz. Dr. med. Matthias Lüke

2. Berichterstatter: Priv.-Doz. Dr. med. Dr. med. dent. Samer Hakim

Tag der mündlichen Prüfung: 01.07.2015

Zum Druck genehmigt: Lübeck, den 01.07.2015

-Promotionskommission der Sektion Medizin-

The effects of Rho-kinase inhibitor H-1152P, the dyes acid violet-17 and indocyanine green on retinal function in the electrophysiological model of the isolated and perfused vertebrate retina

Introduction:

The retina is a highly organized and most metabolically active tissue in the body, converting the light signals into visual information conveyed to the central nervous system (CNS). A growing concern regarding retinal toxicity is raised following the daily use of intraocular dyes as adjuvant operative tool and the intraocular application of the drugs in the modern ophthalmology. Clinically, the retinal function can be evaluated by recording the retinal electrical response (electroretinogram = ERG) to a flash of light. The electroretinogram (ERG) is used to investigate stimulus processing of the photoreceptors and the higher neuronal network of the retina. It allows also the research on the effects of drugs and their possible toxicity on retinal function. Preclinical evaluation of the safety and the neuroprotective potency of drugs are crucial steps in the drug development process. The electrophysiological model of the isolated perfused retina is a well defined and flexible technique to investigate different questions of drug effects directly and exclusively on retina function. The model can test the safety and the neuroprotective potency of drugs which are important steps before their intraocular use. In addition to the electrophysiological testing, the isolated bovine retinas can be removed after the experiments and histological investigations of the retinal preparations can be conducted.

General Methodology:

The electrophysiological model of the isolated perfused retina

The electroretinogram (ERG) of the isolated bovine retina is a sensitive and reliable tool for evaluating effects of the applied drugs on the retina. In our study we have investigated the effects of the Rho-kinase inhibitor H-1152P, a novel vital dye acid violet-17 (AV-17) and indocyanine green (ICG) on retinal function. We tested the effects of substances on the b-wave amplitude because the b-wave amplitude is the most sensitive criterion to detect changes reflecting the integrity of the inner neural network of the retina.

Bovine eyes were obtained from a local slaughterhouse and harvested immediately post-mortem. They were transported in darkness in a serum-free standard medium containing 120 mM NaCl, 2 mM KCl, 0.1 mM $MgCl_2$, 0.15 mM $CaCl_2$, 1.5 mM NaH_2PO_4, 13.5 mM Na_2HPO_4, and 5 mM glucose.

The preparation was carried out in darkness under dim red illumination. Eyes were hemisected at the junction of sclera and cornea. The lens and vitreous body were removed. The posterior eyecup was divided to four sclera-choroid-retina segments and from each segment four circular pieces were obtained using a 7-mm trephine. By gentle shaking the retina was separated from the underlying pigment epithelium. The retina mounted on a supporting mesh and placed in a perfusion chamber located in an electrically and optically insulated box.

Each ERG was recorded in the surrounding nutrient medium via two silver/silver-chloride electrodes on either side of the retina. Perfusion velocity was controlled by a roller pump and set to 1 ml/min.

Temperature was kept constant at 30°C. The perfusing medium was pre-equilibrated and saturated with oxygen and could be monitored by a Clark oxygen electrode. Retinas were dark-adapted, and ERGs were elicited at 5-min intervals using a single white flash for stimulation. The flash intensity was set to 6.3 mlx at the retinal surface using calibrated neutral density filters. The duration of light stimulation (500 ms) was controlled by a timer. ERGs were filtered and amplified (100-Hz high-pass filter, 50-Hz notch filter, 100.000× amplification) using a Grass CP 511 amplifier. Data were processed and converted using an analog-to-digital data acquisition board (NI USB-6221; National Instruments, Austin, TX, USA) and a personal computer. The ERGs were recorded and analysed by DASYLab Professional Version 10.0.0 (National Instruments, Austin, TX, USA), **(Fig. 1).**

Retinas were superfused with serum-free nutrient solution and stimulated repeatedly until stable b-wave amplitudes were recorded. The b-wave amplitude was measured from the through of the a-wave to the peak of the b-wave.

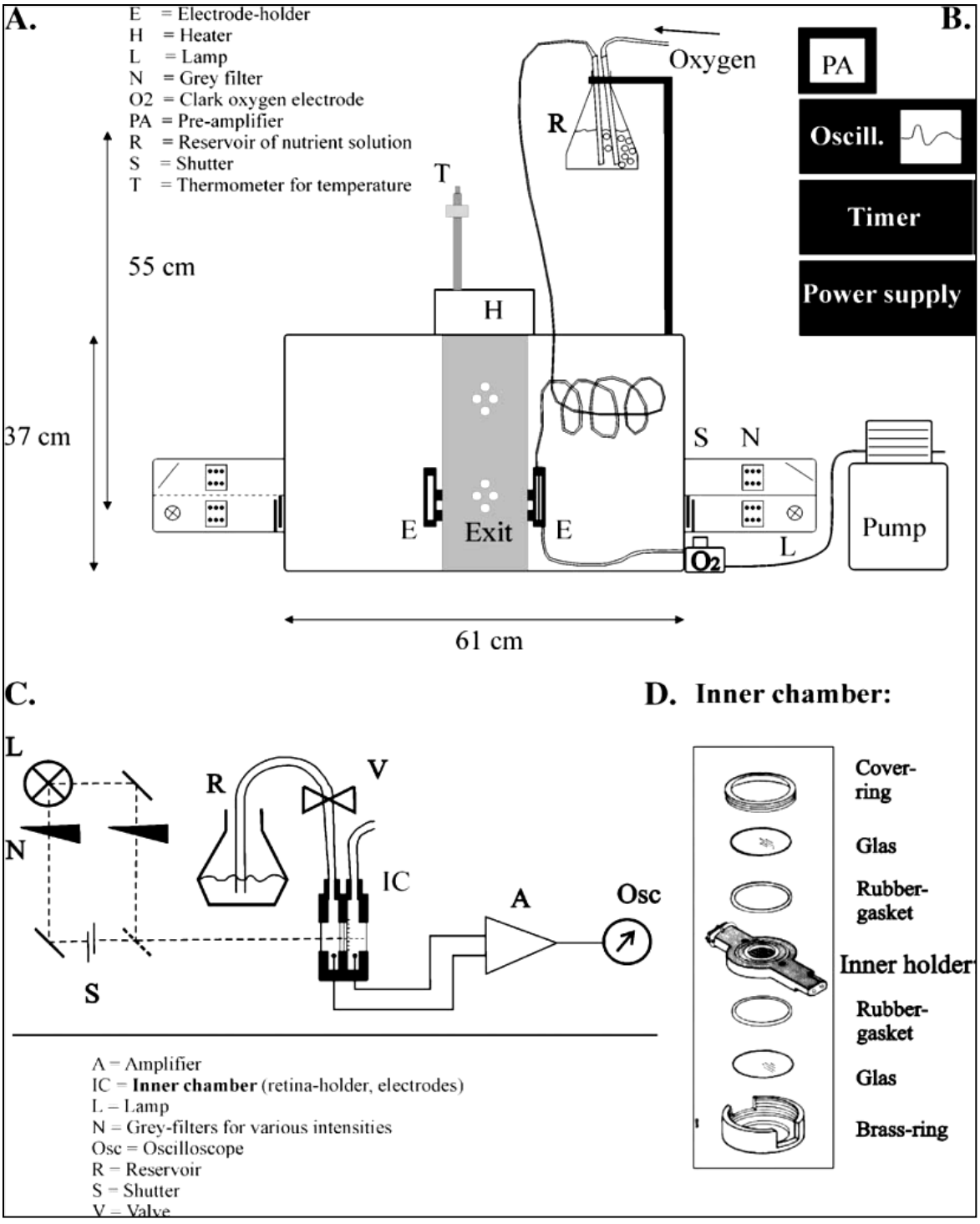

Figure 1. Setup for ERG recording from the isolated perfused bovine retina (A) Overview of the Faraday cage with two separate incubation boxes for perfusion chambers. (B) Stimulation and recording unit. (C) Scheme of the optical and electrical circuits for the ERG recording from the perfused retina. (D) Components of the perfusion chamber.

Live/Dead assay

Retinas followed after ERG-measurements and cultured retinas were incubated for 30 minutes in 4 µM Ethidium homodimer-1 (EthD-1) diluted in 0.1% glucose-PBS, rinsed briefly with 0.1% glucose-PBS twice, fixed with 2% paraformaldehyde (PFA)-PBS for 15 minutes followed by 4% PFA-PBS for 15 minutes. After three rinses in PBS for 5 minutes, the retinas were permeabilized in 0.1% Triton X-100/PBS for 10 minutes and counterstained with DAPI (1 µg/ml in PBS) for 10 minutes to detect the nuclear morphology. The retinas were rinsed twice in PBS, mounted in Mowiol, and analysed by fluorescence. Quantification of the stained cells was performed using the ImageJ software. Data are presented as the mean ± standard error of mean (SEM).

Immunohistochemistry on paraffin sections

The retinas were fixed in formalin, embedded in paraffin, sectioned at 6 µm on a microtome and mounted on Fisherbrand SuperFrost Plus glass slides. After deparaffinization in xylol for three times for 5 minutes and rehydration in a graded series of alcohol descending from 100% to 50%, the slides were rinsed with PBS and blocked with PBS containing 3% BSA and 0.3% Triton X-100 (BSA-PBST) for 30 minutes at room temperature (RT). The sections were incubated with the primary antibodies diluted in the blocking buffer overnight at 4 °C. Negative controls were incubated in the blocking buffer alone. The sections were rinsed in PBS and incubated with the fluorescent-secondary antibodies. The nuclei were counterstained with DAPI (1 µg/ml in PBS) for 5 minutes and the slides mounted with Mowiol were analysed by fluorescence microscopy.

I**mmunohistochemistry on flat-mounted retinas**

For the immunohistochemical detection of microglial reactivity in the nerve fiber layer flat-mounted retinas were fixed in paraformaldehyde and washed three times for 1 h in PBS containing 0.2% Triton X-100. After blocking in 3% BSA-PBST overnight at 4°C, the retinas were incubated with the antibodies against CD11b or GFAP for 48 h at 4°C whereas the negative controls were incubated with the blocking buffer alone. Retinas were washed in PBS three times for 1 h each and incubated with the secondary antibodies indicated above overnight at 4°C. The nuclei were counterstained with DAPI for 10 minutes and the retinas were analysed by fluorescence microscope.

Quantification of microglia reactivity

The morphological quantification of microglia reactivity on the images of the flat-mounted retinas was performed by calculating form factor 1 (FF1) and form factor 2 (FF2). Briefly, the form factor 1 (FF1) is derived from the following equation:

$$\mathbf{FF1} = 4\pi \mathbf{x} \frac{\mathbf{cell\ area}}{(\mathbf{cell\ perimeter})\mathbf{2}}$$

The form factor 2 (FF2) was calculated from the following ratio:

$$FF2 = \frac{\mathbf{cell\ area}}{\mathbf{convex\ area}}$$

For each retina, the mean FF1 and FF2 values of the quantified cells were calculated and for each treatment group as well.

Immunoblotting

The retinas were rinsed briefly in PBS and homogenized in ice-cold tissue lysis buffer (50 mM Tris-HCl, pH 7.4, 2 mM MgCl2, 1% NP-40, 10% glycerol, 100 mM NaCl, and 1% protease and phosphatase inhibitor cocktails added just before use) using 40 µl buffer per retina. The total lysates were cleared by centrifugation at 12000g for 20 minutes. The protein concentration of the supernatant was determined using the BCA assay according to the manufacturer's instructions. Five µg of protein was run in 5-12% denaturing and non-reducing gels at a constant voltage of 120 V for 1-1.5 hours and transferred onto nitrocellulose membranes using a semi-dry blotting apparatus at 25 V for 30 minutes. Ponceau S staining was carried out to verify equal protein loading. Immunoblotting and signal detection by enhanced chemiluminescence were performed, by incubating the membranes with the primary antibodies against cathepsin-B, GFAP, or vimentin overnight at 4°C followed by horseradish peroxidase-conjugated secondary anti-rabbit or anti-mouse antibodies for 1 h at RT.

Experimental layout and statistical analysis

Statistical analysis was done using the SAS System 9.2 for Windows 7 (X64VSPRO, SAS Institute, Cary, NC, USA) and "Origin 6.0" (Microcal) software. For statistical evaluation we fitted two ANOVA models to the data and Student's t- test. $P < 0.05$ was considered as statistically significant.

Study (1):

Publication:

The neuroprotective potential of Rho-kinase inhibition in promoting cell survival and reducing reactive gliosis in response to hypoxia in isolated bovine retina, Aizhan Alt, Ralf-Dieter Hilgers, Aysegül Tura, Khaled Nassar, Toni Schneider, Arno Hüber, Kai Januschowski, Salvatore Grisanti, Julia Lüke, Matthias Lüke. Cellular Physiology and Biochemistry 2013; 32: 218-234

Methods:

To evaluate the outcomes of Rho-kinase inhibition in an ex-vivo model of retinal hypoxia we used a most specific Rho-kinase inhibitor H-1152P. Bovine retinas were perfused with an oxygen saturated nutrient solution with or without the Rho-kinase inhibitor H-1152P and stimulated repeatedly until stable amplitudes were reached and the electroretinogram was recorded at five minutes intervals. To induce hypoxia the oxygen supply was stopped for 15, 30, and 45 minutes and nitrogen was added to the nutrient solution. Subsequently the oxygen saturation was restored. The Rho-kinase inhibitor was applied at the concentrations of 1 or 5 µM to the nutrient solution. The extent of the cell damage and glial reactivity was determined by live/dead staining, immunohistochemistry, and Western blot. Retinal specimens were stained for Cathepsin-B, CD11b, cleaved caspase-3, GFAP and Vimentin. The nuclei were evaluated with DAPI for both Ethidium homodimer-1 staining and for formalin fixed paraffin embedded sections.

Results:

During 15 minutes of hypoxia no considerable effects of the b-wave amplitude were observed. Longer periods of hypoxia (30 and 45 minutes) caused a time-dependent reduction of the b-wave amplitudes, which could not be prevented by the H-1152P. However, a full recovery of the b-wave was observed at the end of the washout, **(Fig. 2).**

Hypoxia also resulted in an increase in cell damage and the activation of the glial cells in the untreated retinas whereas the administration of H-1152P significantly reduced the extent of these events, **(Fig. 3).** The induction of hypoxia resulted in a notable increase in the levels of cytoplasmic Cathepsin-B after 45 minutes. However,

the administration of H-1152P could suppress the leakage of Cathepsin-B into the cytoplasm, which was also confirmed by the immunoblots of the total retinal lysates.
The induction of hypoxia for 15 minutes did not result in a considerable difference in the upregulation of GFAP pattern in either the untreated or the treated retinas. However, the longer exposure to hypoxia led to the significant upregulation of GFAP. In contrast, the administration of the Rho-kinase inhibitor (1μM and 5μM) considerably interfered with the upregulation of GFAP particularly in the Müller cells after a hypoxic period of 30 and 45 minutes. Similarly, the intermediate filament vimentin was significantly upregulated in the untreated retinas after 30 minutes of hypoxia, whereas the treatment with 1 μM H-1152P reduced the level of vimentin. Upregulation of the GFAP and vimentin after 45 minutes of hypoxia and the H-1152P dependent decrease in this process was also confirmed by immunoblotting.
The glial reactivity detected by the immunostainings for the microglia marker CD11b on the retinal flat mounts was preserved in the retinas treated with 1 μM H-1152P after all the hypoxic periods. These findings were also confirmed by the morphological quantifications of the microglia based on the form factors FF1 and FF2, **(Fig. 4).**

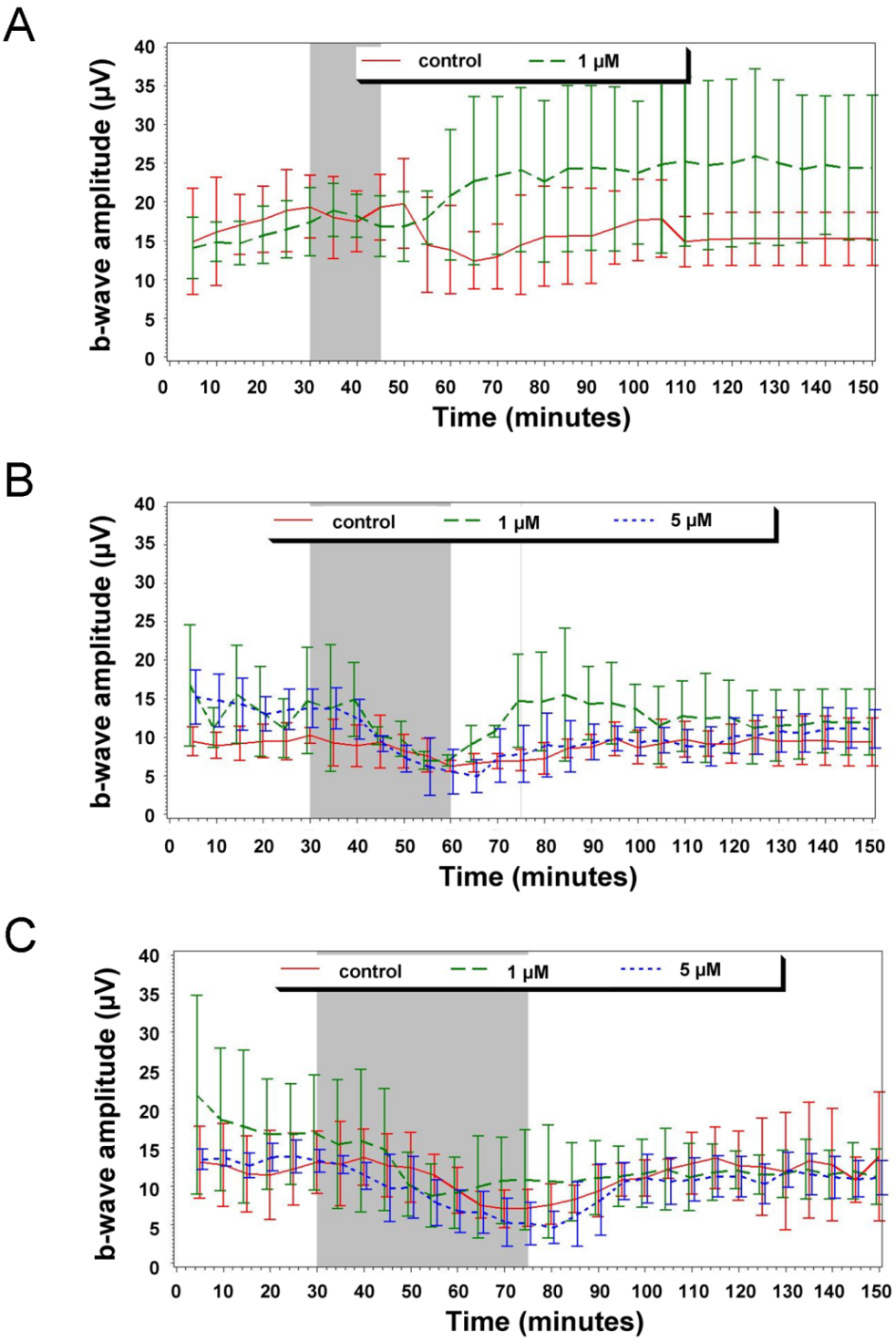

Figure 2. Effects of hypoxia and H-1152P on the course of the electroretinogram. The dashed lines mark the experiments with continuous application of H-1152P compared to the control. The grey background marks the duration of hypoxia.

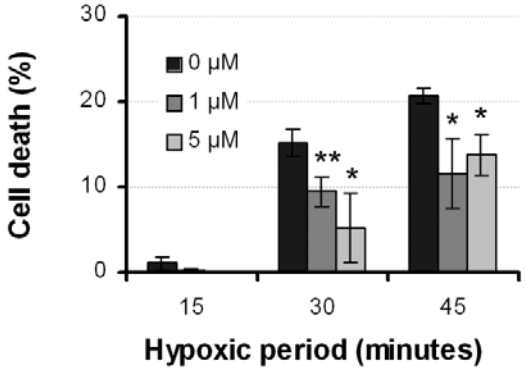

Figure 3. The neuroprotective effect of the Rho-kinase inhibitor in the ganglion cell layer of hypoxic retinas. The administration of the Rho-kinase inhibitor could significantly reduce the percentage of dead cells compared to control without a considerable difference between the concentrations of 1 µM and 5 µM.

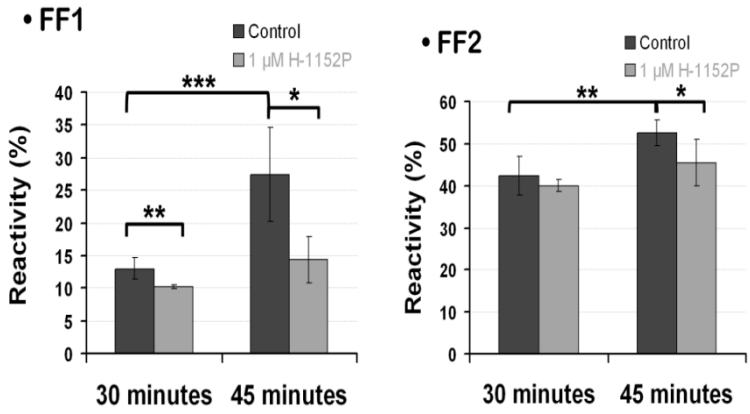

Figure 4. Decrease in the microglial reactivity in response to the Rho-kinase inhibitor.

Conclusion:

Our work provides further support to the neuroprotective potential of the pharmacological Rho-kinase inhibitor H-1152P under hypoxic conditions. However, the inhibitor could not prevent the hypoxia induced retinal dysfunction.

Study (2):

Publication:

Testing the effects of the dye Acid violet-17 on retinal function for an intraocular application in vitreo-retinal surgery. Aysegül Tura, *Aizhan Alt*, Christos Haritoglou, Carsten H. Meyer, Toni Schneider, Salvatore Grisanti, Julia Lüke, Matthias Lüke.
Graefes Arch Clin Exp Ophthalmol. 2014 Dec; 252(12):1927-37

Methods:

In this work we tested the effects of a novel trityl dye Acid violet-17 and its solvent carrier containing D_2O on retinal function and on the retinal cultures. The retina was superfused with the serum-free "nutrient solution" and stimulated repeatedly until stable amplitudes were recorded. Thereafter, the dye solution with solvent carrier at different concentrations or the solvent carrier alone was applied epiretinally. The duration of retinal exposure was varied between 30 seconds and 5 minutes (30, 60, 120 and 300 seconds). After application of the dye solution (0.0125%, 0.025% or 0.05%) the preparation was reperfused with standard solution for at least 130 minutes.

After the same preparation of bovine eyes the retinas were gently dissociated from the underlying pigment epithelium and transferred on to the cellulose nitrate filter in the Petri dish prefilled with fresh HBBS supplemented with calcium and magnesium. Pieces of retina with the underlying cellulose nitrate filter were dissected using a 6-mm biopsy punch along a radius of approximately 1 cm from the central retina. The retinal pieces and the underlying filter were transferred on to culture inserts with a pore size of 0.4 µm placed into a 6-well plate (n=2 retinas/insert). The wells were prefilled with 1 ml of culture medium (Neurobasal-A supplemented with 1X B-27, 1% BSA, 1 mM L-Glutamine, 100 Units/ml penicillin, 100 µg/ml streptomycin, 50 ng/ml BDNF, 20 ng/ml CNTF, denoted as N+). A few drops of culture medium were also pipetted into the inserts at a volume barely sufficient to cover the retinas. The retinas were allowed to recover overnight in a 37°C incubator with 5% CO_2 and humidity.

On the following day, a new 6-well plate was prepared by filling the wells with 1 ml of fresh culture medium and placing new inserts of 0.4 µm pore size into each well. The retinas were placed on to the new inserts. The test substances (AV-17 at a concentration range of 0.0625-0.5 mg/ml; solvent; culture medium) were carefully pipetted into the inserts at a volume of 500 µl/insert, avoiding the detachment of the

retinas from the filter underneath and ensuring that the ganglion cell layer was covered by the test substance. Retinas were incubated in duplicates with the test substances for 30 seconds or 5 minutes. Afterwards, the retinas were washed three times for 5 minutes with sterile PBS and placed back on to the initial culture inserts. The culture medium in each well of the initial culture plate was replenished 1:1 (v/v) with fresh medium and the retinas were incubated overnight at 37°C as described above to allow for recovery.

To determine the outcomes of the exposure to the dye or its solvent on the viability of the cells in the ganglion cell layer, cultured retinas were incubated with AV-17 (at a concentration range of 0.0625-0.5 mg/ml) or the solvent alone for 30 seconds or 5 minutes in duplicates. Retinas exposed to the fresh culture medium for 30 seconds or 5 minutes and washed similarly as the other treated retinas were included as controls. The extent of the cell damage and glial reactivity was determined by live/dead staining, immunohistochemistry and Western blot.

Results:

The solvent carrier including the heavy water did not induce a significant effect on the b-wave amplitude. Application of the dye AV-17 at the concentration of 0.25 mg/ml led to a direct reduction of the b-wave amplitude, which was most prominent after the exposure time of 30 seconds and 120 seconds. The exposure times of 60 and 300 seconds led to a not significant reduction of the b-wave amplitudes, **(Fig. 5).** A full recovery of the b-wave amplitude was reached on an average of 20-25 minutes after applying AV-17.

The application of the AV-17 at a higher concentration of 0.5 mg/ml induced a significant reduction of the b-wave amplitude. The effects on the b-wave amplitude were partially reversible at the end of the washout, but the impairment of full recovery did not reach the level of significance.

Exposure of the lower concentrated AV-17 (0.125 mg/ml) for 5 min induced a not significant reduction of the b-wave amplitude and its fast recovery at the end of the washout.

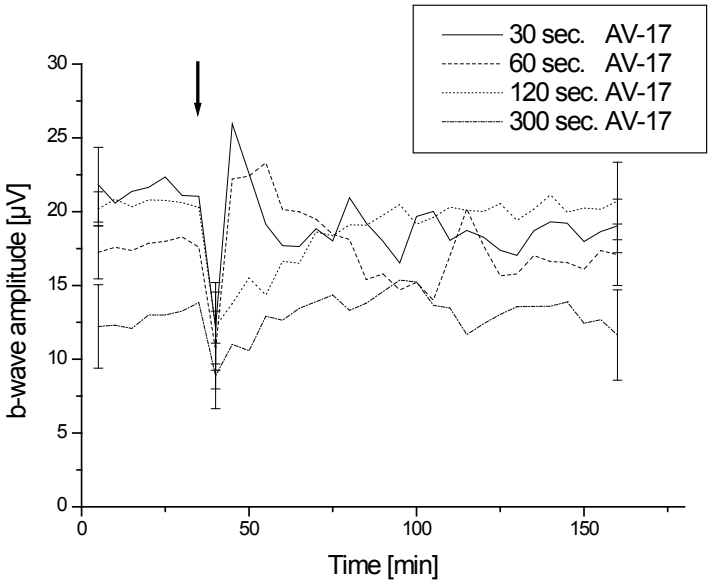

Figure 5. Effects of 0.25 mg/ml AV-17 on the b-wave amplitude of the isolated perfused bovine retina. Average of representative test series. The black arrow marks the application of solvent carrier. Only the retinal exposure time was varied as indicated in the panel. A representative standard deviation for the test series is given.

Exposure to the dye at the concentrations of 0.0625 mg/ml and 0.125 mg/ml was well tolerated by the retinal cells in term of the cellular viability. With increasing concentrations of the dye (0.25 and 0.5 mg/ml), we observed a considerable decrease in viability after the 5-minute exposure to the dye compared to the retinas treated with the solvent alone.

However, a slight increase in GFAP-expression and fiber thickness was observed after the application of the dye at an intermediate concentration of 0.125 mg/ml. Exposure to AV-17 at a concentration of 0.5 mg/ml resulted in a relevant upregulation in the GFAP levels as opposed to all the other groups.

Exposure of the cultured retinas to the dye at the concentrations of 0.0625 and 0.125 mg/ml for 5 minutes led to the slight upregulation of GFAP in the nerve fiber layer and Müller cells. With increasing concentrations of the dye (0.25 and 0.5 mg/ml), the upregulation of GFAP became more prominent even after an exposure of 30 seconds. The retinas treated with the solvent alone for 5 minutes exhibited a very low degree of GFAP-immunoreactivity. The majority of the microglia in the retinas exposed to AV-17 at the concentrations of 0.125 and 0.5 mg/ml also exhibited a ramified morphology. However, the number and length of these protrusions were

gradually reduced with increasing concentrations of the dye for the group treated with 0.5 mg/ml AV17 for 5 minutes.
The solvent carrier was very well tolerated not only in terms of cell survival in the ganglion cell layer but also the extent of glial reactivity, resulting in no considerable activation of the astrocytes, Müller cells or the microglia compared to the normal retinas treated with medium.

Conclusion:
Application of AV-17 at a concentration of up to 0.125 mg/ml in a D_2O-carrying solvent was well tolerated in terms of retinal function, survival in the GCL, and glial reactivity and appears safe for intraocular administration. The extent of viability in the ganglion cell layer was reduced after the long-term exposure to the dye at high concentrations together with an increase in glial reactivity.

Study (3):
Publication:
The concentration dependent effects of indocyanine green on retinal function in the electrophysiological ex-vivo model of the isolated perfused vertebrate retina, Mahdy Ranjbar, *Aizhan Alt*, Khaled Nassar, Mihaela Reinsberg, Toni Schneider, Salvatore Grisanti, Julia Lüke, Matthias Lüke. Ophthalmic Res. 2014;51(3):167-71

Methods:
In this work we evaluated the effects of a dye indocyanine green (ICG) at different concentrations on retinal function in the model of isolated superfused bovine retina. The retina was superfused with the serum-free nutrient solution and stimulated repeatedly until stable amplitudes were recorded. The standard medium was replaced by ICG at the concentration of 0.025%, 0.0025%, 0.00025 and 0.000025% for 45 minutes. For each concentration of ICG a new isolated retina was used. Afterwards the preparation was reperfused with standard medium for at least 85 minutes. Additionally, we tested ICG at the concentration of 0.05% for 21 seconds

Results:
During exposure of ICG at the concentration of 0.025% and 0.0025% for 45 minutes we found a significant reduction of the b-wave amplitude. Exposure of lower

concentrated ICG (0.00025% and 0.000025%) did not have any statistically significant impact on the ERG, **(Fig. 6).**

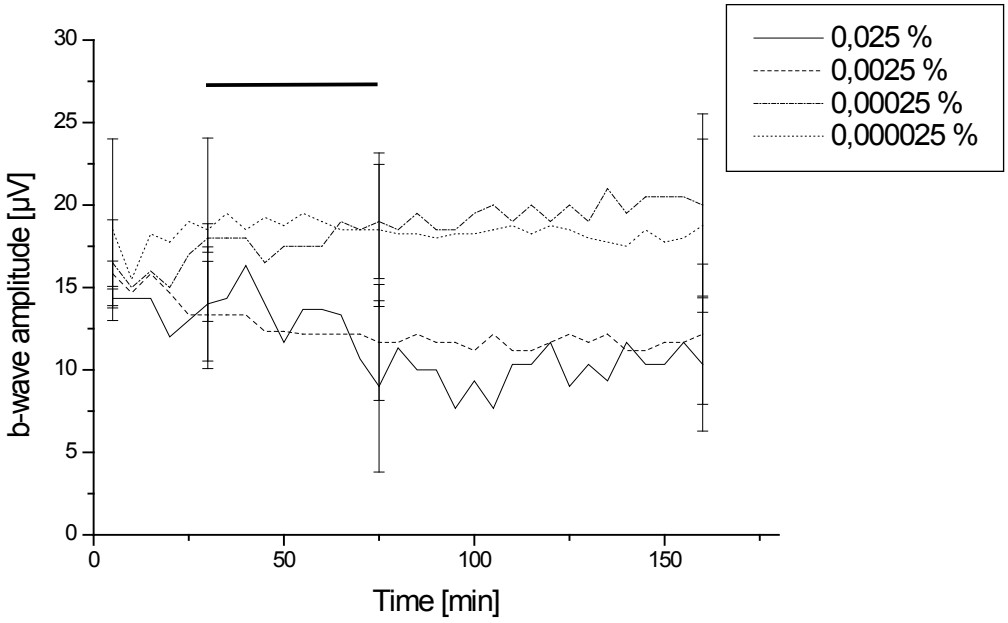

Figure 6. Effects of ICG at the different concentrations for 45 min on the b-wave amplitude of the isolated perfused bovine retina. Effects of ICG on the b-wave amplitude of the isolated perfused bovine retina. Average of representative drug series. The horizontal bar marks the application of the indicated different concentrations for 45 min. A representative standard deviation for the test series is given.

The effects of ICG at the concentration of 0.0025% on the ERG were reversible at the washout, whereas at the concentration of 0.025% the b-wave amplitude still remained decreased within the recovery time. The lower tested concentrations did not lead to a significant deficiency of b-wave recovery during the washout, **(Tabl.1).**
The exposure of ICG at a concentration of 0.05% for 21 seconds led to highly significant reduction of the b-wave amplitude by abolishing the responses directly after exposure. However, at the end of the washout a partial recovery was observed, in which the b-wave amplitude was not significant different to the amplitudes prior to exposure.

ICG-concentration	PBR (SD) [%]	p-value
0.025%	-27.7 (9.6)	0.0082**
0.0025%	-10.4 (10.0)	0.1917
0.00025%	+6.6 (28.5)	0.9142
0.000025%	+11.1 (25.9)	0.7509

Table 1. ERG results 85 minutes after ICG exposure and reperfusion with standard medium in the meantime; PBR: persistent b-wave reduction; SD: standard deviation

Conclusion:

ICG at the concentration of 0.025% or higher have persistent effects on retinal function. Lesser concentrations might be safe, but are not sufficient for the visualization of ILM.

English summary

The electroretinogram (ERG) of isolated and perfused bovine retina is a sensitive tool for testing effects of applied drugs and substances on retina function. However, using the isolated retina corresponds most closely to the situation in vivo where the substance is directly applied on retinal surface during vitreoretinal surgery.

With this model of isolated retina it is possible to provide stable ERG recordings for at least 10 h. In our electrophysiological model we tested different drugs: Rho-kinase inhibitor H-1152P, novel vital dye Acid violet-17 (AV-17) and indocyanine green (ICG).

Our experiments provide further support to the neuroprotective potential of the pharmacological Rho-kinase inhibitor H-1152P under hypoxic conditions. The retina is very sensitive to hypoxic stress, which occurs in variety of pathological conditions in the eye, such as diabetic retinopathy, choroidal neovascularisation, age-related macular degeneration and vascular occlusions. Several research investigations are focused on developing of strategies and neuroprotective substances aimed at preventing the death of neurons and the restoration of the normal function under such unfavourable conditions. Yet, no clinical trial has shown neuroprotective efficacy

of the tested agents in the ocular diseases until now, which necessitates the identification of novel cellular targets central to the pathological processes induced by hypoxia in the retina. In our experiments we tested Rho-kinase inhibitor, as a Rho-kinase inhibition increased the retinal cell survival under different injury paradigms in the retina including NMDA-induced neurotoxicity, serum deprivation, optic nerve crush, and transient retinal ischemia. The selective inhibition of Rho-kinase therefore appears as a very efficient strategy to achieve concurrently the multiple aspects of neuroprotection in the retina, such as the prevention of neurite retraction, promotion of neuronal survival, suppression of excessive glial reactivity which might otherwise result in detrimental effects on the rescued neurons, and the maintenance of the retinal blood flow. However, the outcomes of Rho-kinase inhibition on retinal function under hypoxia have not been elucidated yet.

Our study showed that the presence of the inhibitor did not prevent the functional decrease during the hypoxic phase or promote a faster recovery during the reperfusion. However, the cells treated with the inhibitor were significantly protected from damage and are expected to function properly once the normal conditions are restored. The inhibitor could therefore be applied during hypoxic conditions to restrict the extent of retinal damage especially in the ganglion cell layer, which could have a clinical significance.

Vital dyes improve the visualisation of less recognizable structures like epiretinal membranes or the internal limiting membrane (ILM) during macular surgery. The aim of our study was to investigate the biocompatibility of a new dye, acid violet-17 (AV-17) and indocyanine green (ICG) on retinal function, using the electrophysiological ex-vivo technique of the isolated superfused bovine retina model.

A reduction of the ERG amplitudes of the isolated perfused vertebrate retina was noticed after the application of AV-17 for all test series. However, this effect could not be interpreted as a toxic effect and can be explained by the absorption of the applied light via the dye. Moreover, a recovery was observed after application for all test series at the washout. Exposure to the dye at the lower concentrations was well tolerated by the retinal cells in terms of the cellular viability in the ganglion cell layer and the maintenance of glial cells in a quiescent state. However, some remarkable effects on cell viability at the higher concentrations were found. This was associated with the activation of astrocytes and Müller cells, providing further evidence to the ongoing retinal stress. Based on our results we conclude that the application of AV-

17 at a concentration of 0.125mg/ml or below in a D_2O-carrying solvent appears safe for intraocular administration. Nevertheless, restricting the time the retina is exposed to this novel dye would be advisable to avoid adverse effects through excessive glial reactivity.

Our investigations regarding the effects of ICG revealed an exposure time and also a concentration dependent impact of ICG at the concentrations of 0.025% or higher on retinal function in an isolated, superfused retina model. Lesser concentrations regarding the ERG might be safe, but are not clinically applicable caused by the decreasing staining ability. Therefore, the continuous use of ICG in macular surgery should be taken into question, because a safe ICG solution with sufficient staining properties might not exist.

The ERG model of isolated perfused retina is a sensitive and well defined screening method for new drugs. Moreover, the drug concentration which reaches the retina is close to the intraoperative situation in human macular surgery. In conclusion, our findings provide further support to the neuroprotective potential of the Rho-kinase inhibition under hypoxic conditions, the application of AV-17 at a concentration of 0.125 mg/ml or below appears save and the application of ICG at a concentrations of 0.025% or higher have persistent effects on retinal function.

Deutsche Zusammenfassung

Die Effekte des Rho-kinase-Inhibitors H-1152P, sowie der Farbstoffe Acid-violet-17 und Indocyaningrün auf die retinale Funktion im elektrophysiologischen Modell der isolierten und umströmten Vertebratennetzhaut

Das Elektroretinogramm (ERG) der isolierten und umströmten Rindernetzhaut ist eine sensitive Testmethode, um die Effekte der applizierten Substanzen beziehungsweise Wirkstoffe auf die retinale Funktion testen zu können. Dieses Modell ermöglicht es, die Wirkstoffeffekte auf die retinale Funktion gezielt zu untersuchen, unabhängig von systemischen Stoffwechselprozessen, wie es am lebenden Tier zutrifft.

Der experimentelle Aufbau des Modells der isolierten und umströmten Vertebratennetzhaut entspricht besonders der klinischen Situation in vivo, bei der Substanzen intraoperativ teilweise direkt auf die Netzhautoberfläche gegeben werden. Innerhalb dieses Modells ist es möglich, die isolierte Netzhaut über mehr als 10 Stunden am Leben zu erhalten, ohne einen signifikanten Verlust der Amplitudenhöhe der ERG-Messung beobachten zu können. Im Rahmen der vorgelegten Dissertation erfolgte in unserem elektrophysiologischen Modell die Testung unterschiedlicher Substanzen: des Rho-kinase-Inhibitors H-1152P und der beiden Farbstoffe Acid-violet-17 (AV-17) und Indocyaningrün (ICG). Unsere Experimente konnten weitere Hinweise liefern, dass der Wirkstoff Rho-kinase-Inhibitor H-1152P einen neuroprotektiven Effekt unter Hypoxie entfalten kann. Die Netzhaut wiederum ist sehr sensibel gegenüber Hypoxie- induziertem Stress. Dies ist Grundlage verschiedenster pathologischer Situationen im Auge, wie es insbesondere die diabetische Retinopathie, die Entwicklung der chorioidalen Neovaskularisation im Rahmen der Makuladegeneration, sowie okuläre Gefäßverschlüsse darstellen.

Eine Vielzahl klinischer Untersuchungen zielten darauf ab, neuroprotektive Wirkstoffe zu entwickeln, die die Apoptose von Neuronen verhindern sollen beziehungsweise eine Wiederherstellung einer normalen Funktion von Neuronen nach einer Minderversorgung wie es die Hypoxie darstellt, herbeizuführen. Doch konnten in bisher keiner klinischen Studie wesentliche neuroprotektive Effekte der bisher untersuchten Medikamente gefunden werden. Daher ist es erforderlich, Wirkstoffe zu erforschen und zu untersuchen, die neue Ansätze auf zellulärem Niveau anbieten

und in die pathologischen Prozesse der Netzhaut unter Hypoxie eingreifen. Eine solche Substanz stellt der Rho-kinase-Inhibitor H-1152P dar.

In Experimenten hatte sich gezeigt, dass die Rho-kinase-Inhibition zu einem verbesserten Überleben retinaler Neuronen geführt hatte, welches bei NMDA induzierter Neurotoxizität bei retinaler Ischämie sowie in Sehnervenkompressions-versuchen nachgewiesen werden konnte.

Die selektive Inhibition der Rho-kinase stellt daher möglicherweise einen sehr effizienten Weg dar, eine Neuroprotektion der Netzhaut zu bewirken, die Apoptose von Neuronen einerseits und sekundäre Veränderungen, wie z.B. die exzessive gliale Reaktivität, andererseits zu vermeiden. Eine Untersuchung der Wirkung der Rho-kinase-Inhibition auf die retinale Funktion unter Hypoxie war bisher noch nicht untersucht worden.

Unsere Studie zeigte, dass eine durch die Hypoxie induzierte retinale Funktionsstörung auch in Anwesenheit des Rho-kinase-Inhibitors nicht verhindert und auch die Erholung während der Reperfusionsphase nicht beschleunigt werden konnte. Jedoch zeigte sich in den histologischen Untersuchungen, dass die Netzhäute, welche mit dem Rho-kinase-Inhibitor H-1152P inkubiert worden waren, signifikant weniger durch Hypoxie induzierte Apoptose aufweisen. Dementsprechend konnte der Inhibitor in der Phase der Hypoxie das Ausmaß des retinalen Schadens reduzieren, wobei dies insbesondere auf der Ebene der Ganglienzellen beobachtet werden konnte, was speziell im Rahmen retinaler Gefäßverschlüsse von besonderer klinischer Bedeutung sein könnte.

Die Farbstoffe AV-17 und ICG werden zur Visualisierung wenig gut darstellbarer Strukturen, wie z.B. der epiretinalen Gliose oder auch der Membrana limitans interna in der Makulachirurgie, benutzt. Ziel unserer Studien war es, die Biokompatibilität sowohl des neuen Farbstoffes AV-17 und von ICG auf die retinale Funktion in unserem Modell der isolierten und umströmten Vertebratennetzhaut zu testen. Die Reduktion der ERG-Amplituden während der Inkubation in unserem Modell, konnte in allen experimentellen Versuchen gezeigt werden. Diese Amplitudenreduktion während der Inkubation kann allerdings nicht als toxischer Effekt an sich gewertet werden, sondern erklärt sich aus der Absorption der Lichtreize durch den Farbstoff. Sobald wiederum der Farbstoff aus der Perfusionskammer herausgespült worden war, zeigte sich eine vollständige Erholung des ERGs in allen Untersuchungsreihen und bei allen applizierten Konzentrationen. Ebenso zeigten die histologischen

Untersuchungen, insbesondere bei den niedrigen Konzentrationen, die getestet worden waren, nach wie vor eine gute Vitalität der Zellen auf Ebene der Ganglienzellschicht. Ebenso kam es nicht zu einer glialen Zellreaktion. In den höheren Konzentrationen, die getestet worden waren, zeigten sich für den Farbstoff AV-17 allerdings deutliche Veränderungen in Bezug auf die Zellviabilität. Diese zeigte eine Aktivierung von Astrozyten und Müllerzellen, was wiederum als Hinweis gedeutet werden kann, dass es zu einer retinalen Stresssituation gekommen war. Basierend auf unseren Resultaten auch im Zusammenhang mit den histologischen Aufarbeitungen der inkubierten Netzhäute in unserem experimentellen Modell, konnte die Konzentration 0.125 mg pro ml in Zusammenhang mit dem getesteten Trägermediums, welches auch schweres Wasser (D_2O) enthält, als für die intraokulare Gabe als sicher bewertet werden. Allerdings muss darauf hingewiesen werden, dass nicht nur die Applikation einer Konzentration entscheidend ist für die Entwicklung der möglicherweise toxischen Effekte auf die retinale Funktion bzw. auf die retinalen Zellen durch einen Farbstoff, sondern ebenso auch die Inkubationszeit. Wird diese entsprechend kurz gehalten, ist die Entstehung von Nebenwirkungen aufgrund der Applikation des Farbstoffes AV-17 unwahrscheinlich.

Entsprechende Beobachtungen konnten in unserer Arbeit bezüglich des ICGs dargestellt werden. So konnte schon in vorherigen Arbeiten gezeigt werden, dass insbesondere die Expositionsdauer eine wichtige Rolle in der Induktion von retinaler Toxizität eine Rolle spielt, aber ebenso scheint diese auch konzentrationsabhängig zu sein. Dabei konnte in unserer Arbeit gezeigt werden, dass auch bisher üblich applizierte Konzentrationen während der Makulachirurgie toxische Effekte auf die retinale Funktion entwickeln können. Erst sehr niedrige Konzentrationen des Farbstoffes ICG scheinen sicher zu sein. Allerdings muss eine Fähigkeit zum Anfärben von intraokularen Strukturen als nicht ausreichend angesehen werden. Basierend auf Untersuchungen muss die Anwendung von ICG in der Makulachirurgie hinterfragt werden, da sichere Konzentrationen von ICG nicht existieren, die auch gleichzeitig eine ausreichende Fähigkeit zur Anfärbung besitzen.

Die vorgelegten Untersuchungen zeigen dementsprechend, dass das Modell der isolierten und umströmten Vertebratennetzhaut sehr sensitiv Effekte auf die retinale Funktion nachweisen kann. Dabei können Situationen simuliert werden, wie sie tatsächlich im Rahmen der klinischen Anwendung intraoperativ existieren. Andererseits lassen sich auch pathophysiologische Situationen simulieren, wie es im

Rahmen unseres Hypoxiemodells der Fall war, so dass z.B. auch Substanzen getestet werden können, die möglicherweise ebenfalls eine neuroprotektive Potenz besitzen. Daher eignet sich unser Modell einerseits, genaue Konzentrationsbereiche für Wirkstoffe anzugeben, in der sie mit hoher Wahrscheinlichkeit keine toxischen Effekte auf die retinale Funktion bewirken beziehungsweise andererseits, dass sich in unserem Modell auch mögliche Eigenschaften von Substanzen nachweisen lassen, wie es die Neuroprotektion darstellt. So konnte für den Farbstoff AV-17 ein sicherer Konzentrationsbereich in der intraokularen Anwendung definiert werden, beziehungsweise für den Farbstoff ICG persistierende Effekte auf die retinale Funktion nachgewiesen werden.

Publications list

Articles:

Alt A, Hilgers R.D, Tura A, Nassar K, Schneider T, Hueber A, Januschowski K, Grisanti S, Lüke J, Lüke M. The neuroprotective potential of Rho-kinase inhibition in promoting cell survival and reducing reactive gliosis in response to hypoxia in isolated bovine retina. Cell Physiol Biochem. 2013;32(1):218-34. doi: 10.1159/000350138. Epub 2013 Jul 26.

Ranjbar M, Alt A, Nassar K, Reinsberg M, Schneider T, Grisanti S, Lüke J, Lüke M. The concentration-dependent effects of indocyanine green on retinal function in the electrophysiological ex vivo model of isolated perfused vertebrate retina. Ophthalmic Res. 2014;51(3):167-71. doi: 10.1159/000357284. Epub 2014 Mar 13.

Tura A, Alt A, Haritoglou C, Meyer CH, Schneider T, Grisanti S, Lüke J, Lüke M. Testing the effects of the dye Acid violet-17 on retinal function for an intraocular application in vitreo-retinal surgery. Graefes Arch Clin Exp Ophthalmol. 2014 Dec;252(12):1927-37. doi: 10.1007/s00417-014-2761-9. Epub 2014 Sep 14.

Presentations:

Tapenbayeva A, Tura A, Lüke J, Lüdeke I.Z, Tolea M, Grisanti S, Lüke M. Die retinale Biokompatibilität von Acid violet-17 im Modell der isolierten und umströmten Vertebratennetzhaut. 109. DOG-Kongress 2011, Berlin. Nr.DO01-008

Posters:

Tapenbayeva A, Tura A, Nassar N, Lüke J, Grisanti S, Lüke M. The neuroprotective potential of Rho-kinase inhibition in promoting cell survival and reducing reactive gliosis under hypoxia in isolated perfused vertebrate retina. ARVO 2011 Annual Meeting, Florida, Poster Presentation, 2650/A131

Nassar K, Tura A, Lüke M, Lüke J, Tapenbayeva A, Grisanti S. Antifibrotic effects of “LY364947”, a potent ATP competitive inhibitor of the TGF-ß type I receptor, on scar formation after glaucoma surgery. ARVO 2011 Annual Meeting, Florida, Poster Presentation, 617/A560

Tapenbayeva A, Hilgers R.D, Tura A, Lüke J, Hüber A, Lüke M. Untersuchung zu den neuroprotektiven Effekten des Rho-Kinase Inhibitors H-1152P zur Verbesserung der retinalen Hypoxietoleranz am elektrophysiologischen Modell der isolierten und perfundierten Vertebratennetzhaut. 109. DOG-Kongress 2011, Berlin, Poster Presentation 385

Tapenbayeva A, Lüke J, Lüke M, Grisanti S, Tura A. Outcomes of Rho-kinase inhibition on the metastatic profile of a uveal melanoma cell line. ARVO 2012 Annual Meeting, Florida, Poster Presentation, 6873/D1203

Acknowledgement :

First and foremost, I would like to express my sincere appreciation and gratitude to my supervisor, Dr. Matthias Lüke, for his unflagging support, continuous encouragement and excellent supervision throughout my work.

I also would like to thank Prof. Dr. Salvatore Grisanti, who welcomed me in the clinic, for providing me the opportunity to conduct my work and his beneficial support.

I would like to thank Prof. Dr. Ralf-Dieter Hilgers for his outstanding help in statistical analysis.

A very special thanks goes out to Dr. Aysegül Tura for her encouragement and sincere friendship. With her immense knowledge and patience she always supported me during my work.

My sincere thanks go to Dr. Dr. Khaled Nassar and Dr. Julia Lüke for offering helpful and constructive discussions, proofreading my thesis and friendly encouragement throughout my work.

I also extend my gratitude to Mrs. Christine Örün for excellent technical assistance.

I am also grateful to Mrs. Petra Hammermeister for all the constructive advice, tremendous support and help over these years.

Finally, I owe my deepest gratitude to my family and my beloved husband Lars for continuous encouragement, love, immeasurable support and unwavering belief in me.

Cellular Physiology and Biochemistry

Cell Physiol Biochem 2013;32:218-234
DOI: 10.1159/000350138
Published online: July 26, 2013
Accepted: July 01, 2013

1421-9778/13/0321-0218$38.00/0

Original Paper

The Neuroprotective Potential of Rho-Kinase Inhibition in Promoting Cell Survival and Reducing Reactive Gliosis in Response to Hypoxia in Isolated Bovine Retina

Aizhan Alt[a] Ralf-Dieter Hilgers[b] Aysegül Tura[a,f] Khaled Nassar[a] Toni Schneider[c] Arno Hueber[d] Kai Januschowski[e] Salvatore Grisanti[a] Julia Lüke[a,f] Matthias Lüke[a,f]

[a]University Eye Hospital, University of Lübeck, Lübeck, Germany; [b]Department of Medical Statistics, RWTH Aachen University, Aachen, Germany; [c]Institute of Neurophysiology, University of Cologne, Köln, Germany; [d]Department of Ophthalmology, University of Cologne, Köln, Germany; [e]Department of Ophthalmology, University Eye Hospital Tübingen, Tübingen, Germany; [f]Contributed equally to this work and should be regarded as equivalent senior authors

Key Words
Electroretinogram • Neuroprotection • H-1152P • Astrocyte • Müller cell • Microglia • Cathepsin-B

Abstract
Aims: To investigate the outcomes of Rho-kinase inhibition in the electrophysiological *ex vivo* model of the isolated perfused vertebrate retina under hypoxia. ***Methods:*** Bovine retinas were perfused with an oxygen saturated nutrient solution with or without the Rho-kinase inhibitor H-1152P. The retinas were stimulated repeatedly until stable amplitudes were reached and the electroretinogram was recorded at five minute intervals. Hypoxia was induced for 15, 30, and 45 minutes, after which the oxygen saturation was restored. The extent of the cell damage and glial reactivity was determined by Ethidium homodimer-1 staining, immunohistochemistry, and Western blot. ***Results*:** Hypoxia caused a time-dependent reduction of the b-wave amplitudes, which could not be prevented by the H-1152P. Although the Rho-kinase inhibitor maintained higher b-wave amplitudes, these effects did not reach statistical significance. Hypoxia also resulted in an increase in cell damage and the activation of the glial cells in the untreated retinas whereas the administration of H-1152P significantly reduced the extent of these events. ***Conclusion:*** H-1152P exerted a neuroprotective effect against necrosis on the isolated bovine retina under hypoxia together with a reduction in glial cell reactivity. However, the inhibitor could not prevent the hypoxia induced retinal dysfunction possibly due to the interference with synaptic modulation.

PD Dr. med. Matthias Lüke

University Eye Hospital, University of Lübeck
Ratzeburger Allee 160, D-23538 Lübeck (Germany)
Tel. +49 451 500 4010, Fax +49 451 500 2945, E-Mail matthias.lueke@uk-sh.de

Introduction

The retina is one of the most metabolically active tissues in the body, consuming large quantities of energy to convert the light signals into a visual information conveyed to the brain [1, 2]. The high-energy demand of particularly the photoreceptors, which respond to the light and the retinal ganglion cells, the axons of which constitute the optic nerve that transmits the visual output to the brain, is fulfilled mainly by the oxygen-dependent generation of adenosine triphosphate (ATP) [3, 4]. This in turn necessitates a constant blood flow through the retinal vasculature and choroid, with the former providing oxygen and nutrients to the ganglion cells and the inner retinal neurons and the latter supporting the photoreceptors in the outer retina [2]. However, the impairment of vascular integrity or haemodynamics can result in the reduction of the oxygen tension below the levels normally present in a cell, tissue, or organism and lead to the state defined as hypoxia. The insufficient oxygen supply would interfere with the metabolic events required for maintaining the homeostasis in the retina and can therefore compromise the cell survival and function particularly after longer durations [2, 5-8]. Hypoxia is indeed associated with a variety of pathological conditions in the eye, such as glaucoma [9, 10], diabetic retinopathy [11], choroidal neovascularisation, and age-related macular degeneration [12, 13], which may severely and irreversibly impair the vision. The development of strategies aimed at preventing the death of neurons and the restoration of the normal function under such unfavourable conditions therefore gains an increasing concern. Although a growing number of neuroprotective agents have yielded positive results in preclinical studies, only a few drugs were examined in human clinical trials [14]. Yet, no clinical trial has shown neuroprotective efficacy in the ocular diseases until now [15], which necessitates the identification of novel cellular targets central to the pathological processes induced by hypoxia in the retina.

Rho-kinase (ROCK1 and ROCK2) is an intracellular serine/threonine kinase that functions as a downstream effector of the RhoA-GTPase, and regulates mainly the assembly of the actin cytoskeleton, which underlies a wide range of cellular responses to the extracellular cues, such as contraction, migration, proliferation, and gene expression [16, 17]. Rho-kinase is best characterized for its role in promoting the contractility of the smooth muscle cells by favouring the phosphorylation of myosin and the formation of the actin-myosin bundles that provide the cells with contractile strength [18]. Accordingly, the suppression of Rho-kinase activity using pharmacological inhibitors like Fasudil and Y-27632 effectively promoted the vasodilation in numerous experimental models [19-21], and the clinical use of the former inhibitor yielded promising results for the treatment of several cardiovascular disorders and subarachnoid haemorrhage in humans [22, 23]. Recent studies also demonstrated an improvement in ocular blood flow at the optic nerve head in response to different Rho-kinase inhibitors [24, 25]. In addition, the selective inhibition of Rho-kinase allowed for the regeneration of the retinal ganglion cell axons in numerous models of optic nerve injury [26-28] and prevented the retraction of the photoreceptor axons in an *in vitro* model of acute retinal detachment [29]. Moreover, an increase in retinal cell survival in response to the Rho-kinase inhibition has recently been demonstrated under different injury paradigms in the retina including NMDA-induced neurotoxicity, serum deprivation, optic nerve crush, and transient retinal ischemia [28, 30-34]. These findings altogether highlight the involvement of Rho-kinase at a convergence point of diverse pathological events that can be associated with hypoxia. The selective inhibition of Rho-kinase therefore appears as a very efficient strategy to concurrently achieve the multiple aspects of neuroprotection in the retina, such as the prevention of neurite retraction, promotion of neuronal survival, suppression of excessive glial reactivity which might otherwise result in detrimental effects on the rescued neurons [31], and the maintenance of the retinal blood flow. However, the outcomes of Rho-kinase inhibition on retinal function under hypoxia have not been elucidated yet.

The synaptic activity within the retina can be evaluated continuously by recording the electroretinogram (ERG) [6]. The b-wave is the ERG-component, which represents the post-photoreceptor activity in the retina and was found to be having the highest degree

of susceptibility to ischemia/hypoxia. Consistently, the recovery of the b-wave depends on the severity of the experimental model and the duration of hypoxia/ischemia. The reduction in the amplitude of the b-wave is therefore regarded as a sensitive indicator of reduced oxygen delivery in humans as well as the *in vivo* and *in vitro* models [6, 35, 36]. In our study, we evaluated the outcomes of Rho-kinase inhibition in an *ex-vivo* model of retinal hypoxia, using H-1152P to modulate the Rho-kinase activity. H-1152P is a dimethylated derivative of fasudil and has the highest degree of specificity among the currently available pharmacological Rho-kinase inhibitors [37]. The ex-vivo effects of Rho-kinase inhibition on the retinal function were determined by monitoring the b-wave amplitudes in isolated and perfused bovine retinas during the hypoxia and reperfusion intervals. Moreover, the retinas were subsequently analysed for the extent of cell survival and glial reactivity to evaluate the outcomes of Rho-kinase inhibition on the cellular responses to hypoxia.

Materials and Methods

Chemicals and reagents

The analysis grade chemicals used for the preparation of the perfusion medium were purchased from Merck (Darmstadt, Germany). H-1152P was purchased from Calbiochem (Merck) and reconstituted in sterile tri-distilled water. The antibodies and the fluorescent reagents used were as follows: Rabbit anti-Cathepsin-B (Acris Antibodies, Herford, Germany), mouse anti-CD11b (Serotec, Düsseldorf, Germany), rabbit anti-cleaved caspase-3 (Cell Signalling Technology, Danvers, MA), rabbit anti-GFAP (DAKO, Hamburg, Germany), mouse anti-Vimentin (Sigma-Aldrich, Munich, Germany), Cy3-conjugated goat anti-rabbit IgG (Jackson Immunoresearch, Dianova, Hamburg, Germany), Alexa 546-conjugated anti-mouse IgG (Molecular Probes, Invitrogen, Darmstadt, Germany), horseradish peroxidase-conjugated secondary anti-rabbit or anti-mouse antibodies (Jackson Immunoresearch). The protease and phosphatase inhibitor cocktails were purchased from Roche Applied Sciences (Mannheim, Germany). All the remaining chemicals were obtained from Sigma-Aldrich.

ERG of isolated perfused bovine retina

Bovine eyes were obtained from a local slaughterhouse and harvested immediately post-mortem. They were transported in darkness in a serum-free standard medium containing 120 mM NaCl, 2 mM KCl, 0.1 mM $MgCl_2$, 0.15 mM $CaCl_2$, 1.5 mM NaH_2PO_4, 13.5 mM Na_2HPO_4, and 5 mM glucose. Our study was in accordance with guidelines from the public health department. Preparations were performed as described previously [38].

Each ERG was recorded in the surrounding nutrient medium via two silver/silver-chloride electrodes on either side of the retina. The recording chamber, containing a piece of retina, was placed in an electrical and optical insulated box. Perfusion velocity was controlled by a roller pump and set to 1 ml/min.

Temperature was kept constant at 30°C. The perfusing medium was pre-equilibrated and saturated with oxygen and could be monitored by a Clark oxygen electrode to demonstrate the hypoxic condition of the nutrient solution. Retinas were dark-adapted, and ERGs were elicited at 5-min intervals using a single white flash for stimulation. The flash intensity was set to 6.3 mlx at the retinal surface using calibrated neutral density filters. The duration of light stimulation (500 ms) was controlled by a timer. ERGs were filtered and amplified (100-Hz high-pass filter, 50-Hz notch filter, 100,000× amplification) using a Grass CP 511 amplifier. Data were processed and converted using an analog-to-digital data acquisition board (NI USB-6221; National Instruments, Austin, TX, USA) and a personal computer. The ERGs were recorded and analysed by DASYLab Professional Version 10.0.0 (National Instruments, Austin, TX, USA).

Retinas were superfused with serum-free nutrient solution and stimulated repeatedly until stable amplitudes were recorded. The oxygen supply into the nutrient solution was stopped for 15 min, 30 min or 45 min and nitrogen was added to the nutrient solution. Meanwhile, the responses were recorded. Thereafter, perfusion with the standard solution was resumed at least for 75 min to monitor b-wave recovery during washout. The b-wave amplitude was measured from the trough of the a-wave to the peak of the b-wave.

To determine the neuroprotective effect of H-1152P we performed the same experimental setup, in which we applied the inhibitor at the concentrations of 1 or 5 μM to the nutrient solution, which was used

for the perfusion of the retinas during the entire measurement period. We studied the effects of H-1152P on ERG parameters varying the time of hypoxia as described before. Recovery of the ERG was followed up for at least 75 min during the washout period. A new retina was used for each experiment with n=5 retinas per group except for the 5 µM H-1152P and the 45-minute hypoxia groups, for which n=4 retinas were used.

Ethidium homodimer-1 staining

Following the ERG-measurements, the retinas were mounted onto cellulose nitrate filters (Sartorius, Göttingen, Germany, 0.45 µm pore size, pre-soaked in 0.01M phosphate buffered saline (PBS) and cut into approximately 1x1 cm pieces) with the ganglion cell layer exposed. The retinas were incubated for 30 minutes in 4 µM Ethidium homodimer-1 (EthD-1) (Molecular Probes) diluted in 0.1% glucose-PBS, rinsed briefly with 0.1% glucose-PBS twice, fixed with 2% paraformaldehyde (PFA)-PBS for 15 minutes followed by 4% PFA-PBS for 15 minutes. After three rinses in PBS for 5 minutes, the retinas were permeabilized in 0.1% Triton X-100/PBS for 10 minutes and counterstained with DAPI (1 µg/ml in PBS) for 10 minutes to detect the nuclear morphology. The retinas were rinsed twice in PBS, mounted in Mowiol, and analysed by fluorescence microscopy (Leica, Wetzlar, Germany). Quantification of the stained cells was performed in 8-10 areas of 0.16 mm^2 per retina using the Image J software (National Institutes of Health, Bethesda, Maryland, USA, http://imagej.nih.gov/ij/, 1997-2012) Image J. Data are presented as the mean ± standard error of mean (SEM).

Immunohistochemistry on paraffin sections

The retinas were fixed in formalin, embedded in paraffin, sectioned at 6 µm on a microtome (Leica, Model RM2125RT) and mounted on Fisherbrand SuperFrost Plus glass slides (Fisher Scientific, Houston, TX). After deparaffinization in xylol for three times for 5 minutes and rehydration in a graded series of alcohol descending from 100% to 50%, the slides were rinsed with PBS and blocked with PBS containing 3% BSA and 0.3% Triton X-100 (BSA-PBST) for 30 minutes at room temperature (RT). The sections were incubated with the primary antibodies diluted in the blocking buffer overnight at 4 °C. Negative controls were incubated in the blocking buffer alone. The sections were rinsed in PBS and incubated with the fluorescent-secondary antibodies. The nuclei were counterstained with DAPI (1 µg/ml in PBS) for 5 minutes and the slides mounted with Mowiol were analysed by fluorescence microscopy (Leica).

Immunohistochemistry on flat-mounted retinas

For the immunohistochemical detection of microglial reactivity in the nerve fiber layer of flat-mounted retinas, the protocol of Wang et al. [39] was performed with slight modifications. Briefly, the flat-mounted retinas were fixed in paraformaldehyde as above and washed three times for 1 h in PBS containing 0.2% Triton X-100. After blocking in 3% BSA-PBST overnight at 4°C, the retinas were incubated with the antibodies against CD11b diluted 1/5 in the blocking buffer for 48 h at 4°C whereas the negative controls were incubated with the blocking buffer alone. Retinas were washed in PBS three times for 1 h each and incubated with the secondary antibodies indicated above overnight at 4°C. The nuclei were counterstained with DAPI for 10 minutes and the images were acquired under 400x magnification using a fluorescence microscope (Leica).

Quantification of microglia reactivity

The morphological quantification of microglia on the images of the flat-mounted retinas was performed by calculating two different form factors as described [40]. Briefly, the form factor 1 (FF1) is derived from the following equation:

$$FF1 = 4\pi \times \frac{\text{cell area}}{(\text{cell perimeter})^2}$$

The FF1 ratio yields values between 0 and 1, acquiring the latter value for a perfectly round (ameboid) cell and decreasing as the number and/or length of the ramifications, hence the cell perimeter increases. The FF1 is therefore a sensitive indicator of initial ramification, acquiring lower values with the presence of even very short cytoplasmic processes. However, it does not always reflect the true degree of microglia reactivity, since an oval shaped cell without ramifications also gets a considerably lower FF1 value compared

to the round, reactive microglia [40]. For this purpose, we also quantified the microglia reactivity in terms of the FF2, which was calculated from the following ratio:

$$FF2 = \frac{\text{cell area}}{\text{convex area}}$$

The convex area is the area of a polygonal object defined by the cell's most prominent and extended projections. For an ameboid (reactive) cell, both the normal and the convex areas would have similar values and the FF2 approaches 1, whereas the long ramifications would significantly increase the convex area, resulting in the reduction of the FF2 ratio [40]. The FF2 values therefore serve as a more specific indicator for the true, long ramifications. Quantification of the microglia area, perimeter, and the convex area was performed individually for each cell using the Image J software on a minimum number of n=16 cells/retina that were entirely localized within the boundaries of an image. The FF1 and FF2 ratios were calculated as above individually for each cell and denoted as percentage. For each retina, the mean FF1 and FF2 values of the quantified cells were calculated. For each treatment group, the mean ± SEM of the FF1 and FF2 values were calculated from the individual mean values obtained from n=3 independently processed retinas per group.

Immunoblotting

The retinas were rinsed briefly in PBS and homogenized in ice-cold tissue lysis buffer (50 mM Tris-HCl, pH 7.4, 2 mM $MgCl_2$, 1% NP-40, 10% glycerol, 100 mM NaCl, and 1% protease and phosphatase inhibitor cocktails added just before use) using 40 µl buffer per retina. The total lysates were cleared by centrifugation at 12000g for 20 minutes. The protein concentration of the supernatant was determined using the BCA assay (Pierce, Rockford, IL) according to the manufacturer's instructions. Five µg of protein was run in 5-12% denaturing and non-reducing gels at a constant voltage of 120 V for 1-1.5 hours and transferred onto nitrocellulose membranes using a semi-dry blotting apparatus (Biotec-Fischer, Reiskirchen, Germany) at 25 V for 30 minutes. Ponceau S staining was carried out to verify equal protein loading. Immunoblotting and signal detection by enhanced chemiluminescence were performed as described previously [31], by incubating the membranes with the primary antibodies against cathepsin-B (1:1000), GFAP (1:2000), or vimentin (1:1500) overnight at 4°C followed by horseradish peroxidase-conjugated secondary anti-rabbit or anti-mouse antibodies (1:2500) for 1 h at RT.

Experimental layout and statistical analysis

The experimental layout results in data from 8 experimental groups. There are three different hypoxia times (15, 30 and 45 minutes) and three different concentrations for the Rho-kinase inhibitor H-1152P: 0 µM (control group), 1 µM, and 5 µM. However, in the 15 minutes hypoxia group, the high dose of H-1152P (5µM) was not applied. Within each group measurements were taken every 5 minutes from 5 (start of experiment) up to 150 minutes. The first six measurements before hypoxia were used as baseline measurements, followed by the group specific time of hypoxia and by a follow-up period of 105 minutes in the 15 minutes hypoxia group or 75 minutes in the 45 minutes hypoxia group.

For statistical analysis we used the last baseline measurement (30 minutes), last measurement under hypoxia (45, 60 or 75 minutes) and the maximal comparable follow-up time (120 minutes for 15 minutes hypoxia, 135 minutes for 30 minutes hypoxia and 150 minutes for 45 minutes hypoxia). We fitted two ANOVA models to the data. Our first model (Model 1) involves the dose 1 µM and control only. Hereby we assume unstructured covariance and the exploratory between grouping factors substance (control, 1µM) and hypoxia duration (15, 30 and 45 minutes) and the within grouping factor hypoxia-status (before, at the end of hypoxia, at the end of recovery). The second model (Model 2) is used to analyse the high dose effect, so we assume an AR(1) covariance structure and use the model building between grouping factors substance (control, 1µM, 5µM) and hypoxia duration (30 and 45 minutes) and the within grouping factor hypoxia-status (before, at the end of hypoxia, at the end of recovery). During fitting we performed a model diagnostic as well. To describe the data, we calculated the percent changes of the b-wave amplitudes after hypoxia or after recovery respectively from baseline. Differences between the b-wave after recovery as well as between the post-hypoxia and baseline or between the experimental series at the different concentrations and the control were analysed by linear contrasts. The statistical significance of the damaged cells in the ganglion cell layer was analysed by two factor main effects ANOVA models followed by linear contrasts on main

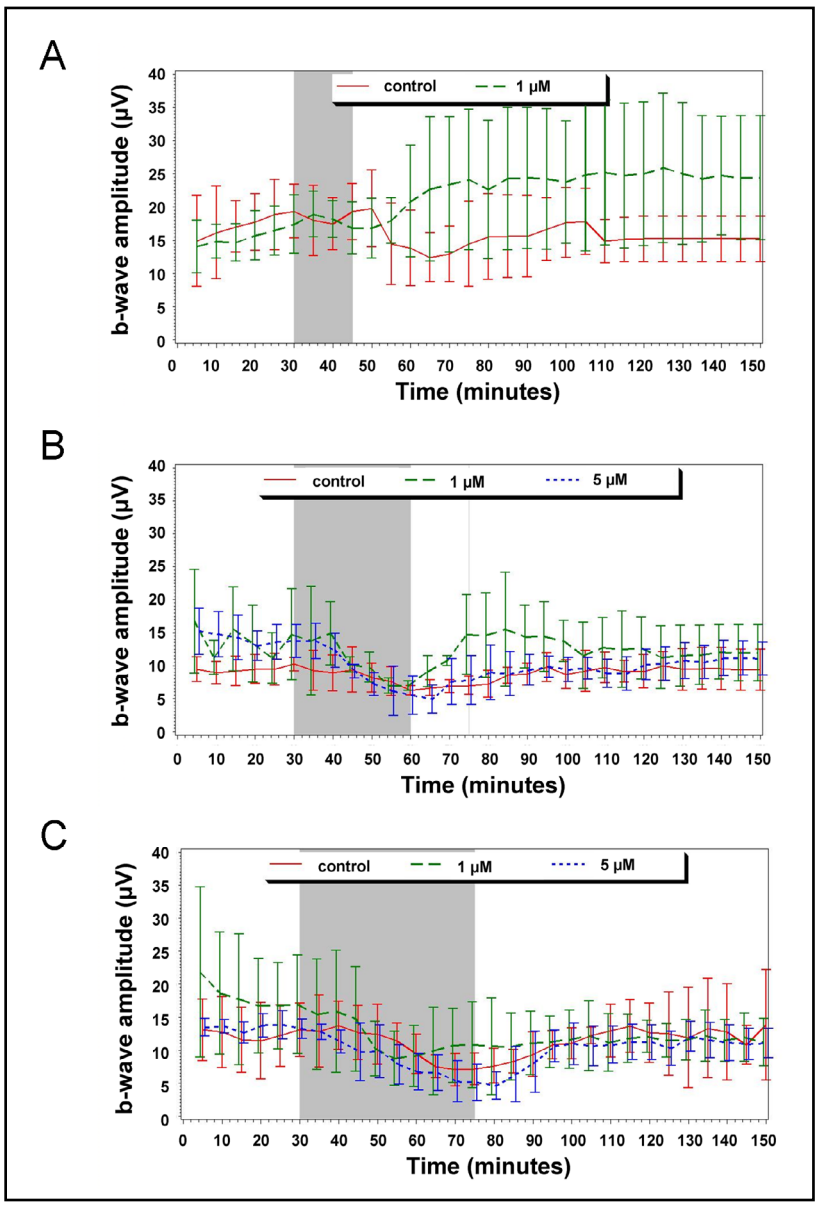

Fig. 1. Effects of hypoxia and H-1152P on the course of the electroretinogram. The figures indicate the course of the b-wave amplitude before and after hypoxia. The dashed lines mark the experiments with continuous application of H-1152P (1 µM and 5 µM, green and blue, respectively) compared to the control (continuous line, red). The grey background marks the duration of hypoxia (A: 15 minutes; B: 30 minutes; C: 45 minutes). Average of representative series. The standard deviation is given for each mean value.

effects. The statistical significance of microglia reactivity was analysed by the two-tailed t-test, assuming equal variance between the samples. Statistical analysis was done using the SAS System 9.2 for Windows 7 (X64VSPRO, SAS Institute, Cary, NC, USA). P-values ≤ 0.05 were assessed as significant.

Results

Functional outcomes of hypoxia for different durations

The perfusion of the isolated bovine retina was performed under stable environmental conditions. Osmotic pressure, temperature, and pO_2 remained unchanged during perfusion.

In our experimental setting stable ERG-amplitudes were reached within two hours perfusion and the superfused retinal preparations responded constantly to light stimulation for more than ten hours [38].

Our first model shows that the b-wave varies significantly between baseline, under hypoxia and at the end of recovery ($F=21.23$, ndf 2, ddf 24, $p<0.0001$, Fig. 1A-C). Furthermore, the mean b-wave changes significantly depending on the duration of hypoxia ($F=10.98$, ndf

2, ddf 24, p=0.0004, Fig. 1A-C) and these two factors interact significantly with each other (F=4.25, ndf 4, ddf 24, p=0.0097, Fig. 1A-C). We observed no significant difference in the course of these events in response to the Rho-kinase inhibitor compared to the untreated retinas (F=1.44, ndf 1, ddf 24, p=0.2422, Fig. 1A-C).

To be more specific, we observed a significant mean change in b-wave from baseline to the last measurement under hypoxia (t=6.33, df 24, p<0.0001, Fig. 1A-C) and from the last measurement under hypoxia to the last observation under recovery (t=-2.65, df 24, p=0.0139, Fig. 1A-C), but no difference between baseline and recovery (t=0.70, df 24, p=0.4904, Fig. 1A-C). Hereby the mean change between baseline and the last measurement under hypoxia is mainly caused by the difference in the 45 minutes group (1 µM: t=5.25, df 24, p<0.0001; control group: t=4.10, df 24, p=0.0004, Fig. 1C) and the 30 minutes group (1 µM: t=5.14, df 24, p<0.0001; control group: t=3.98, df 24, p=0.0005, Fig. 1B).

After recording the stable b-wave amplitudes for 30 minutes, hypoxia was induced by applying nitrogen to the nutrient solution (Fig. 1A). During 15 minutes of hypoxia, the b-wave amplitudes were reduced from 19.35 µV (SD 4.07) to 15.2 µV (SD 3.43) in the untreated retinas (t=-0.50, df 24, p = 0.6224) and increased from 17.4 µV (SD 4.45) to 25.0 µV (SD 10.85) during the additional application of 1 µM H-1152P to the nutrient solution (t=-0.87, df 24, p=0.3935). However, the period of hypoxia was not long enough to induce a considerable effect on the b-wave amplitude (t=0.70, df 24, p=0.4904).

Longer periods of hypoxia (30 and 45 minutes) resulted in progressively greater decreases of the b-wave amplitude (Fig. 1B and 1C). To be more concrete, after 30 minutes of hypoxia, we detected a significant decrease of the b-wave amplitudes from 10.2 µV (SD 1.04) to 6.2 µV (SD 0.69) (t=5.13, df 24, p=0.0005), which was fully reversible at the end of the washout to 9.55 µV (SD 3.14) (t=0.93, df 24, p=0.3624). The application of 1 µM H-1152P did not prevent the reduction of the b-wave amplitude during 30 minutes of hypoxia and we detected a significant decrease of b-wave amplitudes from 14.7 µV (SD 6.91) to 6.95 µV (SD 0.74) (t=5.14, df 24, p < 0.0001, Fig. 1B). However, a rapid recovery was observed within 15 minutes of reperfusion and the ERG-amplitudes at the washout (t=0.56, df 24, p=0.5818) reached the level before hypoxia. Yet, the treatment with 1 µM H-1152P did not improve the course of the b-wave amplitudes compared to the control retinas (F=1.44, ndf 1, ddf 24, p=0.2422).

After 45 minutes of hypoxia (Fig. 1C), the b-wave was significantly reduced from 13.1 µV (SD 4.09) to 7.1 µV (SD 2.40) (t=3.98, df 24, p = 0.0005), but a full recovery of the b-wave amplitudes to 13.80 µV (SD 8.39) (t=1.18, df 24, p=0.2511, compared to baseline) was observed at the end of the washout, which was comparable to the untreated retinas. Administration of H-1152P at 1 µM could not prevent a significant decrease of the b-wave from 16.9 µV (SD 7.48) to 10.8 µV (SD 6.50) (t=5.14, df 24, p < 0.0001) during hypoxia.

Our second model aims to compare the efficacy of different doses of the Rho-kinase inhibitor under hypoxia for 30 and 45 minutes (Fig. 1B and C). We observed, that the b-wave varies significantly between baseline, under hypoxia and at the end of recovery (F=47.94, ndf 2, ddf 44, p<0.0001). Therefore, we did not observe any significant difference in the mean b-wave depending on the duration of hypoxia (F=0.29, ndf 1, ddf 20, p=0.5954) or between the different concentrations of the inhibitor (F=0.85, ndf 2, ddf 20, p=0.4424).

A significant effect of hypoxia on the ERG-amplitudes was observed when the concentration of H-1152P was increased to 5 µM (t=6.80, df 44, p<0.0001) and the b-wave amplitude remained significantly reduced at the end of washout (t=3.07, df 44, p=0.0036). After the exposure to the higher concentration the effect of the inhibitor was significantly different compared to the control (t=2.06, df 44, p=0.0452). Though the reduction of the amplitude was lower in the presence of 1 µM H-1152P, this effect was not significant compared to the control (t=1.55, df 44, p=0.1284, Fig. 1B and C), but the b-wave was higher in response to the inhibitor. Moreover, the effect of 5 µM after hypoxia was reversible at the washout (t=0.92, df 44, p=0.3648) in contrast to the control. A reduction of the b-wave amplitude during hypoxia could also not be prevented despite the application of 5 µM H-1152P (t=6.80, df 44, p<0.0001, Fig. 1B and C) and we found a pronounced reduction of

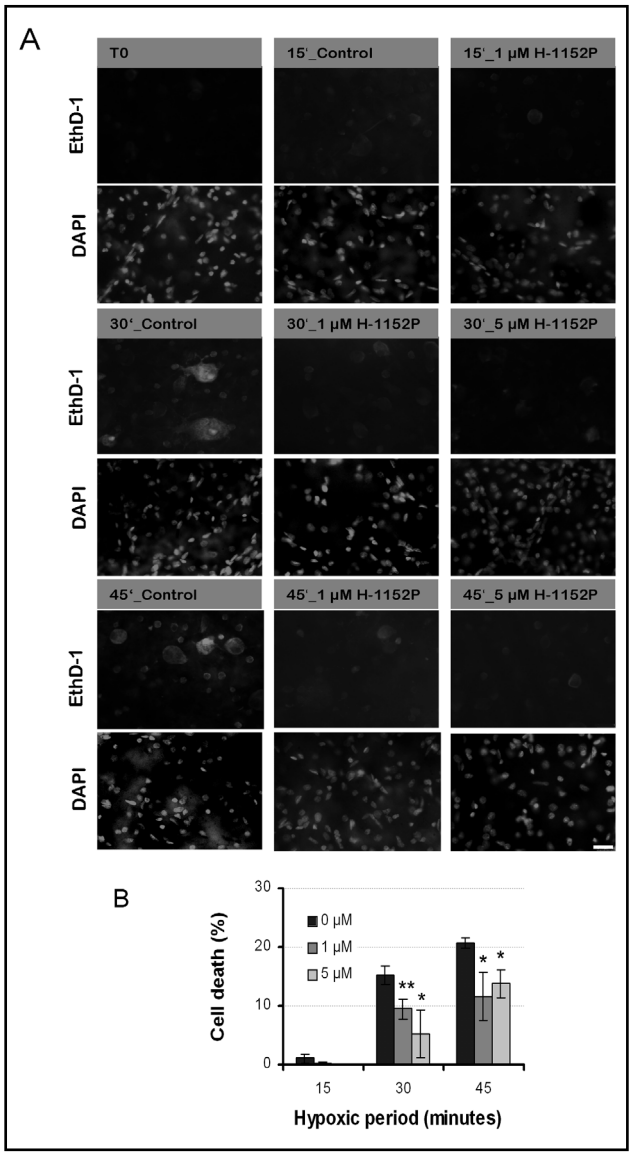

Fig. 2. The neuroprotective effect of the Rho-kinase inhibitor in the ganglion cell layer of hypoxic retinas. (A) Ethidium homodimer-1 (EthD-1) staining performed on the flat mounts of the retinas immediately after the functional measurements. The damaged cells exhibited an increase in the uptake of the fluorescent dye EthD-1. Nuclei were counterstained with DAPI. Hypoxia resulted in a time-dependent increase in the extent of cell damage in the untreated retinas, whereas the treatment with the Rho-kinase inhibitor H-1152P led to a significant reduction in the percentage of dead cells in the ganglion cell layer. Bar indicates 25 µm. (B) Quantification of the percentage of the cell death in the ganglion cell layer after 15 to 45 minutes of hypoxia. Data represent the mean ± SEM of n=2 retinas after 15 minutes of hypoxia and the retinas treated with 5 µM H-1152P during 45 minutes of hypoxia; n=3 retinas for the untreated group (0 µM) during 30 and 45 minutes of hypoxia; n=4 retinas that received 1 and 5 µM of H-1152P during 45 and 30 minutes of hypoxia, respectively; and n=5 retinas treated with 1 µM inhibitor during 30 minutes of hypoxia. *p=0.0006, **p=0.0001.

the b-wave amplitudes compared to the ERG-amplitudes before hypoxia. However, the effect of hypoxia was reversible at the end of the washout.

Reduction in hypoxic cell damage in response to the Rho-kinase inhibitor

Based on the previous studies demonstrating the susceptibility of particularly the retinal ganglion cells to hypoxic conditions [2], we initially focused on the extent of cell survival in the ganglion cell layer as determined by the Ethidium homodimer-1 staining performed on the retinas immediately after the functional measurements. Ethidium homodimer-1 is a cell-impermeable dye that can only enter the cells with damaged membranes, where it undergoes a 40-fold enhancement of red fluorescence upon binding to nucleic acids [41].

We observed no significant difference in the extent of cell damage among the retinas treated with different concentrations of the inhibitor during a given period of hypoxia ($F=0.40$, ndf 2, ddf 21, $p=0.6741$), but a significantly different mean percentage of dead cells depending on the duration of hypoxia ($F=22.11$, ndf 2, ddf 21, $p<0.0001$), with a hypoxic period of 45 minutes resulting in a significant increase in the percentage of dead cells compared to 15 minutes ($t=3.39$, df 21, $p=0.0028$) and 30 minutes ($t=2.64$, df 21, $p=0.0154$).

Furthermore, the mean percentage of dead cells differed significantly between the untreated retinas ($F=35.43$, ndf 2, ddf 2, $p<0.0001$) and the retinas treated with the Rho-

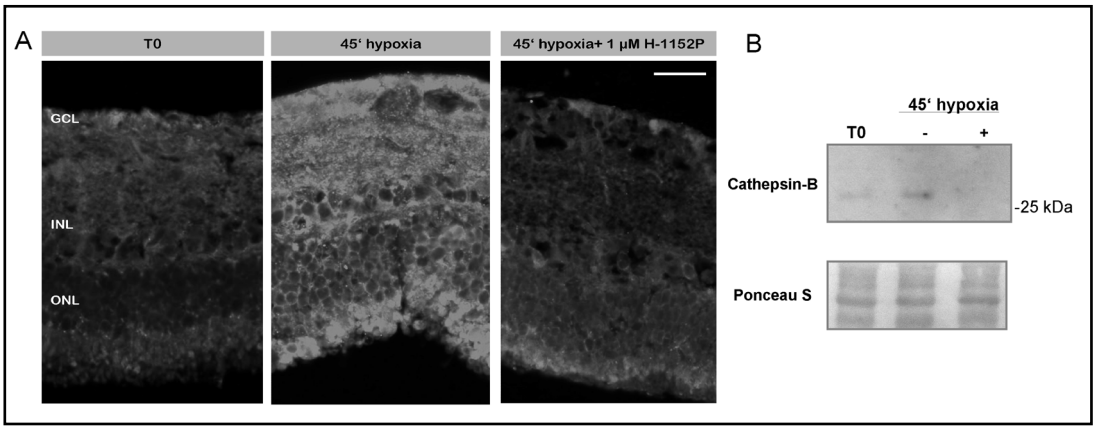

Fig. 3. Changes in the pattern of Cathepsin-B expression after 45 minutes of hypoxia and in response to the Rho-kinase inhibitor. (A) Immunostainings on the paraffin sections of a normal retina at time point 0 (T0) and retinas exposed to hypoxia for 45 minutes with (+) or without (-) 1 µM H-1152P, demonstrating the gradual increase in the levels of the cytoplasmic Cathepsin-B after hypoxia particularly in the ganglion cell layer (GCL) as well as the photoreceptor outer segments underneath the outer nuclear layer (ONL), and the reduction in this process by the Rho-kinase inhibitor. INL: inner nuclear layer. Bar= 25 µm. (B) Representative immunoblot of the whole retinal lysates demonstrating the upregulation of cathepsin-B in response to hypoxia (-) compared to the normal retina at T0. H-1152P (1 µM, +) led to a considerable decrease in the levels of cathepsin-B after 45 minutes of hypoxia. Ponceau S staining was performed to verify equal protein loading.

kinase inhibitor during hypoxia (F=12.94, ndf 2, ddf 20, p=0.0002). Hereby, the prolonged exposure to hypoxia resulted in a gradual increase in the extent of cell damage in the ganglion cell layer, from 1.04 ± 0.7% dead cells after 15 minutes (mean ± SEM of n=2 retinas, t=5.96, df 20, p<0.0001) to 15.17 ± 1.63% dead cells after 30 minutes (mean ± SEM of n=3 retinas, t=8.41, df 20, p<0.0001) and to 20.7 ± 0.85% dead cells after 45 minutes of hypoxia (mean ± SEM of n=3 retinas, t=3.51, df 20, p=0.0022). However, the administration of the Rho-kinase inhibitor could significantly reduce the percentage of dead cells compared to control (t=4.07, df 20, p=0.0006 with 1 µM H-1152P; t=4.68, df 20, p=0.0001 with 5 µM H-1152P) without a considerable difference between the concentrations of 1 µM and 5 µM (t=1.41, df 20, p=0.1729, Fig. 2A and B).

The rupture of the lysosomal membranes and the leakage of the lysosomal enzyme Cathepsin-B into the cytoplasm is a common feature of necrotic cells, which was also observed in different models of hypoxia/ischemia induced neurodegeneration [42-44]. To gain insight into the extent of cell damage in all the retinal layers, we therefore analysed the level of Cathepsin-B in the retinal transverse sections. In the normal retinal pieces fixed immediately after the isolation at time point 0 (T0), we detected a moderate degree of Cathepsin-B immunoreactivity mainly as a cytoplasmic punctate staining in all the cellular layers, consistent with the localization of this protein predominantly to the lysosomes. However, the induction of hypoxia resulted in a notable increase in the levels of cytoplasmic Cathepsin-B after 45 minutes, with a more diffuse expression pattern particularly in the ganglion cells, suggesting the leakage of Cathepsin-B into the cytoplasm. Though the administration of H-1152P could not completely prevent the upregulation of Cathepsin-B under hypoxia, the levels of this protein remained considerably lower particularly in the ganglion cell and photoreceptor layers after 45 minutes of hypoxia in contrast to the untreated retinas. Moreover, the expression pattern of Cathepsin-B in the treated retinas was also mainly punctate similar to the normal retinas at T0, suggesting that the administration of H-1152P could suppress the leakage of Cathepsin-B into the cytoplasm, which was also confirmed by the immunoblots of the total retinal lysates (Fig. 3A and B).

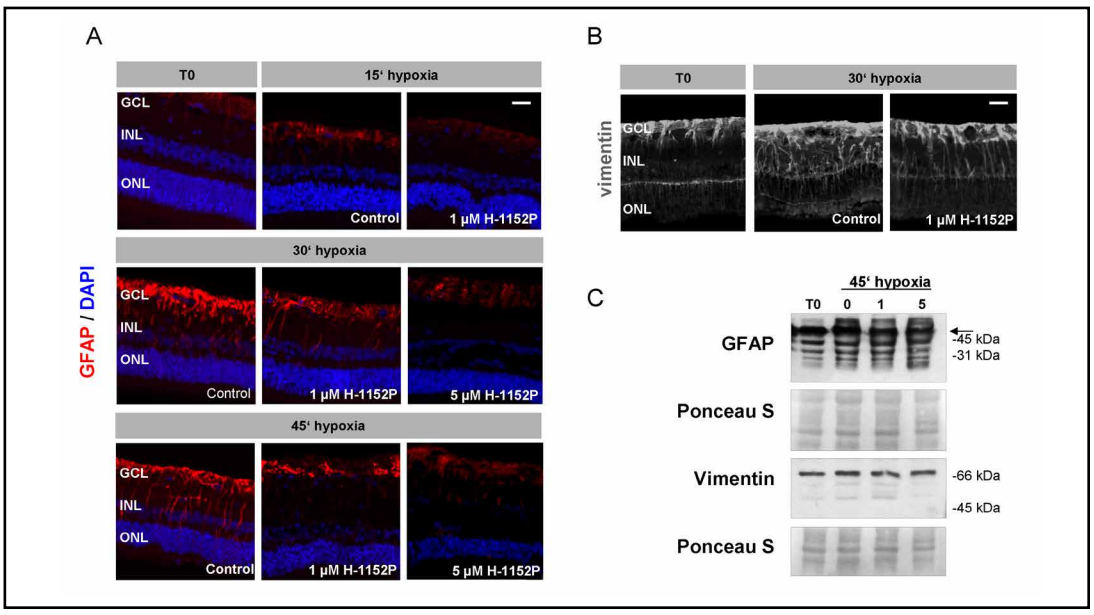

Fig. 4. Decrease in the reactivity of the astrocytes and Müller cells in response to the Rho-kinase inhibitor. (A) Immunostainings for the glial marker GFAP (red) on the paraffin sections of the retinas demonstrating the hypoxia dependent activation of the Müller cells spanning the entire retinal width in the untreated retinas (control) compared to the normal retinas at T0. The elevated GFAP-immunoreactivity in the nerve fiber layer of these retinas (overlaying the GCL) may indicate the bundles of the end-feet of the Müller cells as well as an increase in the reactivity of the astrocytes. In the presence of the inhibitor, the pattern of GFAP immunoreactivity was similar to that observed in the normal retinas at T0, which was confined mainly to the nerve fiber layer with very weak levels of expression in the Müller cell processes extending into the inner nuclear layer (INL). The nuclei were counterstained in blue with DAPI. ONL: outer nuclear layer. (B) Immunostainings for vimentin demonstrating the upregulation of this protein in the Müller cell processes as well as the nerve fiber layer of the untreated retinas after 30 minutes of hypoxia (control), and the H-1152P dependent reduction in this event. (C) Representative immunoblots confirming the upregulation of the main GFAP isoform (49 kDa, indicated by the arrow) and vimentin in response to hypoxia (0) compared to the normal retinas at timepoint 0 (T0). Administration of H-1152P at 1 and 5 µM (1, 5) led to a considerable decrease in the levels of these intermediate filaments after 45 minutes of hypoxia. Ponceau S staining was performed to confirm equal protein loading.

Decrease in hypoxia-dependent glial cell reactivity in response to the Rho-kinase inhibitor

The glial cells execute numerous supportive functions, which are essential for neuronal function and survival. Though the up-regulation of glial reactivity is a rapid response to various stress conditions as a protective attempt, an excessive glial reactivity may exert detrimental effects on the neurons. A common feature of the reactive astrocytes and Müller cells, the radial glia spanning the entire depth of the retina, is the up-regulation of the intermediate filament glial fibrillary acidic protein (GFAP) [45-47]. To determine the extent of astrocyte and Müller cell reactivity in our hypoxia model, we therefore performed immunolabeling for GFAP on the sections of the retina fixed immediately after the reperfusion period.

In the normal retinas at T0, we detected the GFAP-immunoreactivity mainly in the nerve fiber layer where the astrocytes and the end-feet of the Müller cells interact with the ganglion cells. The induction of hypoxia for 15 minutes did not result in a considerable difference in this expression pattern in either the untreated or the treated retinas. However, the 30-minute exposure to hypoxia led to the significant upregulation of GFAP in both the Müller cells extending across the full depth of the retina and in the nerve fiber layer as thick bundles which might represent the aggregated end-feet of the Müller cells as well as the activated astrocytes. This expression pattern was also prevalent after 45-minutes of hypoxia. In contrast, the administration of the Rho-kinase inhibitor (1µM and 5µM) considerably

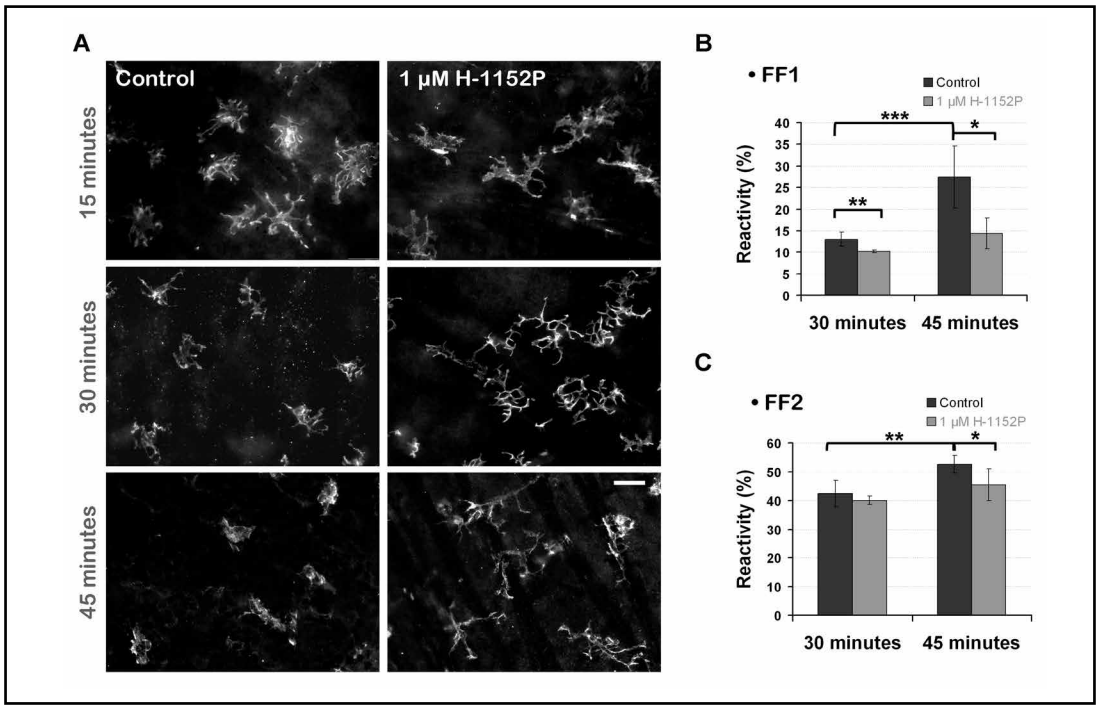

Fig. 5. Decrease in the microglial reactivity in response to the Rho-kinase inhibitor. (A) Morphology of the microglia was determined by the immunostainings for the marker protein CD11b on the flat-mounted retinas immediately after the functional recordings. Hypoxia resulted in the activation of microglia as detected by the gradual retraction of the cellular protrusions and the acquisition of a more ameboid morphology over a period of 45 minutes (control). The Rho-kinase inhibitor H-1152P reduced the extent of microglia reactivity as demonstrated by the maintenance of the long cellular ramifications at all the hypoxic periods tested. Bar indicates 25 µm. (B) Quantification of microglial reactivity based on the form factor 1 (FF1), which reflects the minor differences in the number and/or length of the ramifications. Data represent the mean SEM of n=3 retinas for each group. *p=0.0485, **p=0.0477, ***p=0.0284. (C) Quantification of microglial reactivity based on the form factor 2 (FF2), which is a more specific indicator of true, long ramifications. Data represent the mean SEM of n=3 retinas for each group. *p=0.0177, **p=0.0088.

interfered with the upregulation of GFAP particularly in the Müller cells after a hypoxic period of 30 and 45 minutes (Fig. 4A). Similarly, the intermediate filament vimentin, which is another marker of astrocyte and Müller cell reactivity [47], was significantly upregulated in the untreated retinas after 30 minutes of hypoxia, whereas the treatment with 1 µM H-1152P reduced the level of vimentin in the nerve fiber layer and Müller cells (Fig. 4B). Upregulation of the main GFAP isoform (49 kDa) and vimentin after 45 minutes of hypoxia and the H-1152P dependent decrease in this process was also confirmed by immunoblotting (Fig. 4C).

Hypoxia also resulted in the activation of the microglia in the nerve fiber layer as demonstrated by the immunostainings for the microglia marker CD11b on the retinal flat mounts revealing the cellular morphology [48]. The microglia in the untreated retinas exposed to 15 minutes of hypoxia exhibited the quiescent, ramified morphology. However, as the hypoxic period increased to 30 and 45 minutes, the microglia gradually acquired the reactive, ameboid morphology with the retraction of the protrusions and a decrease in the number of the ramifications. In contrast, the quiescent, ramified microglial morphology was preserved in the retinas treated with 1 µM H-1152P after all the hypoxic periods (Fig. 5A). These findings were also confirmed by the morphological quantifications of the microglia based on the form factors FF1 and FF2, which mainly reflect the low and high degrees of ramification, respectively [40]. In the untreated retinas, the duration of hypoxia resulted in a significant increase in the values of FF1 from 13.00 ± 1.40% after 30 minutes to 27.37 ± 5.89% after 45 minutes (Fig. 5B, mean ± SEM of n=3 retinas for each group, p=0.0284).

Similarly, the FF2 values were increased from 44.67 ± 3.72% after 30 minutes to 59.83 ± 2.50% after 45 minutes of hypoxia in the untreated retinas (Fig. 5C, mean ± SEM of n=3 retinas from each group, p=0.0088), confirming the retraction of the ramifications and the acquisition of a more reactive morphology. In contrast, the microglia in the retinas treated with 1 μM H-1152P had significantly lower FF1 values after both 30 minutes (10.17 ± 0.26%, p=0.0477) and 45 minutes of hypoxia (Fig. 5B, 14.33 ± 2.90%, p=0.0485, mean ± SEM of n=3 retinas for each group). Though we did not observe a significant decrease in the FF2 values of the microglia in the treated retinas after 30 minutes of hypoxia (39.97 ± 1.19%, p=0.1640), the FF2 values of the treated cells after 45 minutes of hypoxia were also significantly lower (Fig. 5C, 45.47 ± 4.60%, p=0.0177, mean ± SEM of n=3 retinas for each group) compared to the microglia in the untreated retinas, demonstrating the suppression of microglia activation by the preservation of both the short and the long, true ramifications in response to the Rho-kinase inhibitor.

Discussion

In our study, hypoxia resulted in a time-dependent reduction of the b-wave amplitudes, which returned to the baseline values during the reperfusion period. This was associated with a significant increase in the extent of cell damage and glial reactivity in the untreated retinas. The Rho-kinase inhibitor exerted a neuroprotective effect in the retinas under hypoxia, with a significant decrease in the amount of the damaged cells and the extent of glial reactivity. Yet, despite the protective effect on the histological level, the inhibitor failed to prevent the hypoxia-dependent functional reduction and did not improve the functional outcome.

Necrosis is the neuronal death mechanism that predominates under conditions of hypoxic/ischemic energy deprivation. However, necrotic events can also activate the components of the apoptotic pathway by energy-independent mechanisms. Accordingly, the combined inhibition of the major cysteine proteases from both the necrotic and the apoptotic pathways is regarded as a more efficient strategy to restrict the neuronal damage after hypoxic/ischemic injury [44]. In our model, the damaged cells exhibited mainly the features associated with necrosis, such as the early decrease in the plasma membrane integrity as detected by the Ethidium homodimer-1 uptake. Though the compromise of the membrane integrity can also be observed at the later stages of the apoptotic cells, our immunostainings for cleaved caspase-3 revealed a very low degree of immunoreactivity in all the treatment groups (data not shown), weakening the possibility that the apoptotic mechanisms were activated at the time points tested. A further support to the hypoxia-dependent necrosis was gathered from the levels of the cytoplasmic Cathepsin-B, a lysosomal cysteine protease which leaks into the cytoplasm due to the rupture of the lysosomal membranes under energy deprivation and may lead to irreversible cell damage through the cleavage of the structural proteins [42-44]. In our model, the leakage of Cathepsin-B in the untreated retinas was prevalent in all the retinal layers after 45 minutes of hypoxia. The absence of the underlying pigment epithelium and the choroid vessels underneath the photoreceptors in the isolated retinas might have resulted in these signs of necrotic damage in the photoreceptors, which are usually not as sensitive as the ganglion cells and the inner retinal neurons in some models of hypoxia/ischemia [2, 49]. Our model therefore simulates a more severe hypoxic condition where not only the retinal vasculature feeding the inner retina, but also the choroid vessels supporting the photoreceptors fail to provide the neurons with oxygen. Nevertheless, despite the adversity of the conditions, the administration of the Rho-kinase inhibitor resulted in a significant reduction in cell damage as indicated by the better preserved plasma membrane integrity. The inhibitor also considerably interfered with the leakage of Cathepsin-B into the cytoplasm, thereby protecting the cells from irreversible damage. Inhibition of Rho-kinase therefore appears to be a simple and efficient strategy to limit the extent of hypoxic cell injury compared to the co-administration of multiple cysteine protease inhibitors.

Rho-kinase is involved in the regulation of the cytoskeletal rearrangements that generate the apoptotic contraction and membrane blebbing [17]. However, the interference with these apoptotic events probably does not underlay the prevailing mechanism of the protective effect of H-1152P in our model, since the damaged cells mainly exhibited the features of necrosis. A likely mediator of cell damage which is targeted by the Rho-kinase inhibitor in our model might be the extracellular glutamate. Glutamate is the major excitatory neurotransmitter in the retina, which is released by the photoreceptors in darkness to activate the bipolar and horizontal cells. The rapid clearance and recycling of glutamate from the synapses is therefore essential for the normal neuronal functioning. The Müller cells are mainly responsible for the glutamate uptake via high affinity transporters, which rely on a very negative membrane potential [50, 51]. However, in retinal ischemia and diabetes, the glutamate uptake into the Müller cells is reduced due to the depolarization of the Müller cells in response to elevated extracellular potassium. The excessive accumulation of glutamate and aspartate in the synapses is implicated in the excitotoxic damage to the retinal ganglion cells. Glutamate excitotoxicity is also a major cause of neuronal loss in the retinal disorders including glaucoma, diabetes, inherited photoreceptor degeneration, and ischemia [52]. Interestingly, the Rho-kinase inhibitor Fasudil could exert a direct neuroprotective effect on primary cerebral neurons through the attenuation of glutamate-induced neurotoxicity [53]. Moreover, glutamate can transiently activate Rho-kinase through the upstream activation of RhoA in hippocampal neurons [54]. These findings favour the possibility that excessive glutamate can also activate the Rho-kinase in the hypoxic retina and the administration of H-1152P can interfere with certain events downstream of glutamate, which remains to be determined.

The protective effect of the Rho-kinase inhibitor might also be related to a reduction in glial reactivity. Indeed, the proliferation and elevated reactivity of Müller cells was associated with the disruption of glutamate recycling in hypoxic retinas in a model of retinal detachment whereas limiting the Müller cell reactivity via oxygen supplementation reduced the abnormalities in glutamate distribution and uptake [55]. H-1152P might have directly interfered with the Müller cell hypertrophy by suppressing the Rho-kinase dependent phosphorylation of GFAP at the head domain and thereby preventing the reorganization of these filaments [56]. Indeed, a novel study demonstrates that several commercially available antibodies against GFAP have a higher affinity towards the phosphorylated protein compared to the unphosphorylated GFAP-isoforms, suggesting that the changes in the levels of GFAP immunoreactivity might in fact reflect the changes in the degree of phosphorylation rather than the total level of this protein [57]. The Rho-kinase may also regulate the cytoskeletal contraction in the microglial cells, resulting in the activation of these cells [31] whereas the inhibitor prevented the transition into the reactive, ameboid morphology. However, the H-1152P dependent decrease in glial reactivity could also have occurred secondarily to the decreased neurotoxicity. Alternatively, the inhibitor might have exerted a direct effect on both the neuronal cells and the retinal glia, resulting in an additive positive outcome on neuronal survival, which remains to be determined.

Yet, the well-preserved cellular integrity and the positive effects on cellular survival in response to H-1152P were not reflected to the functional outcome as estimated by the b-wave amplitudes. H-1152P is an isoquinolinesulfonamide, which structurally resembles adenosine and occupies the ATP-binding domain of Rho-kinase [37]. Interestingly, adenosine can act as a modulator of synaptic transmission in the retina and regulate the blood flow particularly under compromised oxygen delivery [58]. It would be therefore of interest to determine whether H-1152P can interact with the adenosine receptors in the retina, which would have interfered with the synaptic transmission. An alternative reason underlying the inability of the Rho-kinase inhibitor to improve the b-wave amplitudes might be the remodelling of the actin cytoskeleton at the synapses of the depolarizing bipolar cells in an activity dependent manner. The b-wave represents the combined response of the depolarizing bipolar, amacrine, and Müller cells, which are dependent on the hyperpolarization of the photoreceptors upon the perception of light [6, 35]. In response to the light stimulus, the hyperpolarizing bipolar

cells project thin extrusions called spinules into the synaptic processes of the amacrine cells, which possibly strengthens the synaptic connections. In contrast, light causes the retraction of the spinules in the depolarizing bipolar cells concurrent with the formation of filamentous actin in the contracted synaptic pedicles and an increase in protein kinase C (PKC) activity [59]. PKC is indeed a frequently used marker for the bipolar cells, which is localized mainly to the bipolar cell dendrites, axons, and photoreceptor presynaptic terminals, suggesting a key role for PKC in the establishment of the retinal circuitry [60, 61].

The direct inhibition of PKC via H-1152P can be possible *in vitro* using purified molecules, yet the affinity of the inhibitor to other kinases is considerably lower, as reflected by the Ki value of 1.6 nM for the Rho-kinase as opposed to the Ki value of 630 nM for protein kinase A, and 9.27 μM for PKC in cell-free assays [37]. However, the inhibitor is usually administered at micromolar concentrations in cell-based assays, since it has to compete with the intracellular ATP, which is present in millimolar concentrations in most cells [62]. Owing to its high metabolic activity, the retina is particularly rich in ATP, with the concentrations reaching 1 mM in the photoreceptor outer segments of the bovine retina [63]. In our study, we applied the inhibitor at 1 to 5 μM based on a previous study on serum deprived retinas *in vitro*, where the application of H-1152P at 1 μM significantly reduced the Rho-kinase dependent phosphorylation of the cytoskeletal protein adducin without interfering with the PKA-dependent phoshorylation of the same protein [31]. Therefore, the unspecific targeting of PKC in our model remains as a very weak possibility despite the shortage of energy and the reduction in intracellular ATP that the inhibitor will be competing with [64, 65]. Interestingly, PKC can act as an upstream activator of the RhoA/Rho-kinase pathway in diverse cell types [66]. Though the involvement of Rho-kinase in the synaptic remodeling in the retina is to our knowledge not reported, it is likely that the H-1152P could have reversed the actin reorganization in the bipolar cell synapses, resulting in the absence of a functional improvement. Moreover, the majority of significant cell protection by Rho-kinase inhibition was mainly found in the ganglion cell layer in our model. However, the ganglion cell function does not contribute to the course of our recorded electroretinogram. Therefore, a functional improvement due to ganglion cell survival could not be detected in our model although the neuroprotective effect was observed by histological assessment.

In conclusion, our findings provide further support to the neuroprotective potential of the pharmacological Rho-kinase inhibitor H-1152P under hypoxic conditions. Though the presence of the inhibitor did not prevent the functional decrease during the hypoxic phase or promote a faster recovery during the reperfusion, the cells treated with the inhibitor were significantly protected from necrotic damage and are expected to function properly once the normal conditions are restored. Nevertheless, the termination of the treatment soon after the reestablishment of the normal perfusion might be necessary to avoid the possible interference with the synaptic modulation and to thereby restore the neuronal function. The inhibitor could therefore be applied during hypoxic conditions to restrict the extent of retinal damage especially in the ganglion cell layer, which could have a clinical significance in the case of a branch or central arterial retinal occlusion, in which the deterioration of the ganglion cell layer after an arterial occlusion of retina results in a pronounced visual impairment in these patients [67].

Conflict of Interest

All authors have no financial interest related to the manuscript. All authors disclosed any private sponsorship or funding arrangements relating to this research and all authors disclosed any possible conflicts of interest related to this paper.

Acknowledgments

The authors would like to thank Ms. Christine Örün for technical assistance. This work was financially supported by the Research Funding Program/Faculty of Medicine, University of Lübeck (E13-2009).

References

1 Ames A: Energy requirements of CNS cells as related to their function and to their vulnerability to ischemia: a commentary based on studies on retina. Can J Physiol Pharmacol 1992;70:S158-S164.
2 Caprara C, Grimm C: From oxygen to erythropoietin: relevance of hypoxia for retinal development, health and disease. Prog Retin Eye Res 2012;31:89-119.
3 Haugh LM, Linsenmeier RA, Goldstick TK: Mathematical models of the spatial distribution of retinal oxygen tension and consumption, including changes upon illumination. Ann Biomed Eng 1990;18:19-36.
4 Morgan JE: Circulation and axonal transport in the optic nerve. Eye (Lond) 2004;18:1089-1095.
5 Brown JL, Hill JH, Burke RE: The effect of hypoxia on the human electroretinogram. Am J Ophthalmol 1957;44:57-67.
6 Block F, Schwarz M: The b-wave of the electroretinogram as an index of retinal ischemia. Gen Pharmacol 1998;30:281-287.
7 Tinjust D, Kergoat H, Lovasik JV: Neuroretinal function during mild systemic hypoxia. Aviat Space Environ Med 2002;73:1189-1194.
8 Kergoat H, Hérard ME, Lemay M: RGC sensitivity to mild systemic hypoxia. Invest Ophthalmol Vis Sci 2006;47:5423-5427.
9 Osborne NN, Melena J, Chidlow G, Wood JP: A hypothesis to explain ganglion cell death caused by vascular insults at the optic nerve head: possible implication for the treatment of glaucoma. Br J Ophthalmol 2001;85:1252-1259.
10 Flammer J, Orgül S, Costa VP, Orzalesi N, Krieglstein GK, Serra LM, Renard JP, Stefánsson E: The impact of ocular blood flow in glaucoma. Prog Retin Eye Res 2002;21:359-393.
11 Lange CA, Stavrakas P, Luhmann UF, de Silva DJ, Ali RR, Gregor ZJ, Bainbridge JW: Intraocular oxygen distribution in advanced proliferative diabetic retinopathy. Am J Ophthalmol 2011;152:406-412.e3.
12 Harris A, Chung HS, Ciulla TA, Kagemann L: Progress in measurement of ocular blood flow and relevance to our understanding of glaucoma and age-related macular degeneration. Prog Retin Eye Res 1999;18:669-687.
13 Grunwald JE, Metelitsina TI, Dupont JC, Ying GS, Maguire MG: Reduced foveolar choroidal blood flow in eyes with increasing AMD severity. Invest Ophthalmol Vis Sci 2005;46:1033-1038.
14 Whitcup SM: Clinical trials in neuroprotection. Prog Brain Res 2008;173:323-335.
15 Danesh-Meyer HV, Levin LA: Neuroprotection: extrapolating from neurologic diseases to the eye. Am J Ophthalmol 2009;148:186-191.
16 Matsui T, Amano M, Yamamoto T, Chihara K, Nakafuku M, Ito M, Nakano T, Okawa K, Iwamatsu A, Kaibuchi K: Rho-associated kinase, a novel serine/ threonine kinase, as a putative target for the small GTP binding protein Rho. EMBO J 1996;15:2208-2216.
17 Riento K, Ridley AJ: Rocks: multifunctional kinases in cell behaviour. at Rev Mol Cell Biol 2003;4:446-456.
18 Fukata Y, Amano M, Kaibuchi K: Rho-Rho-kinase pathway in smooth muscle contraction and cytoskeletal reorganization of non-muscle cells. Trends Pharmacol Sci 2001;22:32-39.
19 Yao L, Romero MJ, Toque HA, Yang G, Caldwell RB, Caldwell RW: The role of RhoA/Rho kinase pathway in endothelial dysfunction. J Cardiovasc Dis Res 2010;1:165-170.
20 Dong M, Yan BP, Liao JK, Lam YY, Yip GW, Yu CM: Rho-kinase inhibition: a novel therapeutic target for the treatment of cardiovascular diseases. Drug Discov Today 2010;15622-629.
21 Shin HK, Salomone S, Ayata C: Targeting cerebrovascular Rho-kinase in stroke. Expert Opin Ther Targets 2008;12:1547-1564.

22 Satoh K, Fukumoto Y, Shimokawa H: Rho-kinase: important new therapeutic target in cardiovascular diseases. Am J Physiol Heart Circ Physiol 2011;301:H287-H296.
23 Hirooka Y, Shiokawa H: Therapeutic potential of Rho-kinase inhibitors in cardiovascular diseases. Am J Cardiovasc Drugs 2005;5:31-39.
24 Sugiyama T, Shibata M, Kajiura S, Okuno T, Tonari M, Oku H, Ikeda T: Effects of fasudil, a Rho-associated protein kinase inhibitor, on optic nerve head blood flow in rabbits. Invest Ophthalmol Vis Sci 2011;52:64-69.
25 Tokushige H, Waki M, Takayama Y, Tanihara H: Effects of Y-39983, a selective Rho-associated protein kinase inhibitor, on blood flow in optic nerve head in rabbits and axonal regeneration of retinal ganglion cells in rats. Curr Eye Res 2011;36:964-970.
26 Tan HB, Zhong YS, Cheng Y, Shen X: Rho/ROCK pathway and neural regeneration: a potential therapeutic target for central nervous system and optic nerve damage. Int J Ophthalmol 2011;4:652-657.
27 Watanabe M: Regeneration of optic nerve fibers of adult mammals. Dev Growth Differ 2010;52:567-576.
28 Rao VP, Epstein DL: Rho GTPase/Rho kinase inhibition as a novel target for the treatment of glaucoma. BioDrugs 2007;21:167-177.
29 Fontainhas AM, Townes-Anderson E: RhoA inactivation prevents photoreceptor axon retraction in an in vitro model of acute retinal detachment. Invest Ophthalmol Vis Sci 2011;52:579-587.
30 Kitaoka Y, Kitaoka Y, Kumai T, Lam TT, Kuribayashi K, Isenoumi K, Munemasa Y, Motoki M, Kobayashi S, Ueno S: Involvement of RhoA and possible neuroprotective effect of fasudil, a Rho kinase inhibitor, in NMDA-induced neurotoxicity in the rat retina. Brain Res 2004;1018:111-118.
31 Tura A, Schuettauf F, Monnier PP, Bartz-Schmidt KU, Henke-Fahle S: Efficacy of Rho-kinase inhibition in promoting cell survival and reducing reactive gliosis in the rodent retina. Invest Ophthalmol Vis Sci 2009;50:452-461.
32 Lingor P, Tönges L, Pieper N, Bermel C, Barski E, Planchamp V, Bähr M: ROCK inhibition and CNTF interact on intrinsic signalling pathways and differentially regulate survival and regeneration in retinal ganglion cells. Brain 2008;131:250-263.
33 Hirata A, Inatani M, Inomata Y, Yonemura N, Kawaji T, Honjo M, Tanihara H: Y-27632, a Rho-associated protein kinase inhibitor, attenuates neuronal cell death after transient retinal ischemia. Graefes Arch Clin Exp Ophthalmol 2008;246:51-59.
34 Yang C, Lafleur J, Mwaikambo BR, Zhu T, Gagnon C, Chemtob S, Di Polo A, Hardy P: The role of lysophosphatidic acid receptor (LPA1) in the oxygen-induced retinal ganglion cell degeneration. Invest Ophthalmol Vis Sci 2009;50:1290-1298.
35 Coleman K, Fitzgerald D, Eustace P, Bouchier-Hayes D: Electroretinography, retinal ischemia and carotid artery disease. Eur J Vasc Surg 1990;4:569-573.
36 Zager EL, Ames A: Reduction of cellular energy requirements. Screening for agents that may protect against CNS ischemia. J Neurosurg 1988;69:568-579.
37 Sasaki Y, Suzuki M, Hidaka H: The novel and specific Rho-kinase inhibitor (S)-(+)-2-methyl-1-[(4-methyl-5-isoquinoline)sulfonyl]-homopiperazine as a probing molecule for Rho-kinase-involved pathway. Pharmacol Ther 2002;93:225-232.
38 Lüke M, Weiergräber M, Brand C, Siapich SA, Banat M, Hescheler J, Lüke C, Schneider T: The isolated perfused bovine retina – A sensitive tool for pharmacological research on retinal function. Brain Res Brain Res Protoc 2005;16:27–36.
39 Wang L, Cioffi GA, Cull G, Dong J, Fortune B: Immunohistologic evidence for retinal glial cell changes in human glaucoma. Invest Ophthalmol Vis Sci 2002;43:1088-1094.
40 Heppner FL, Roth K, Nitsch R, Hailer NP: Vitamin E induces ramification and downregulation of adhesion molecules in cultured microglial cells. Glia 1998;22:180-188.
41 Boyd V, Cholewa OM, Papas KK: Limitations in the use of fluorescein diacetate/propidium iodide (FDA/PI) and cell permeable nucleic acid stains for viability measurements of isolated islets of Langerhans. Curr Trends Biotechnol Pharm 2008;2:66-84.
42 Kilinc M, Gürsoy-Ozdemir Y, Gürer G, Erdener SE, Erdemli E, Can A, Dalkara T: Lysosomal rupture, necroapoptotic interactions and potential crosstalk between cysteine proteases in neurons shortly after focal ischemia. Neurobiol Dis 2010;40:293-302.
43 Carloni S, Carnevali A, Cimino M, Balduini W: Extended role of necrotic cell death after hypoxia-ischemia-induced neurodegeneration in the neonatal rat. Neurobiol Dis 2007;27:354-361.

44 Unal-Cevik I, Kilinç M, Can A, Gürsoy-Ozdemir Y, Dalkara T: Apoptotic and necrotic death mechanisms are concomitantly activated in the same cell after cerebral ischemia. Stroke 2004;35:2189-2194.
45 Fletcher EL, Downie LE, Hatzopoulos K, Vessey KA, Ward MM, Chow CL, Pianta MJ, Vingrys AJ, Kalloniatis M, Wilkinson-Berka JL: The significance of neuronal and glial cell changes in the rat retina during oxygen-induced retinopathy. Doc Ophthalmol 2010;120:67-86.
46 Tezel G, Wax MB: Glial modulation of retinal ganglion cell death in glaucoma. J Glaucoma 2003;12:63-68.
47 Bringmann A, Wiedemann P: Müller glial cells in retinal disease. Ophhalmologica 2012;227:1-19.
48 Langmann T: Microglia activation in retinal degeneration. J Leukoc Biol 2007;81:1345-1351.
49 Birol G, Wang S, Budzynski E, Wangsa-Wirawan ND, Linsenmeier RA: Oxygen distribution and consumption in the macaque retina. Am J Physiol Heart Circ Physiol 2007;293:H1696-H1704.
50 Bui BV, Hu RG, Acosta ML, Donaldson P, Vingrys AJ, Kalloniatis M: Glutamate metabolic pathways and retinal function. J Neurochem 2009;111:589-599.
51 Bringmann A, Pannicke T, Biedermann B, Francke M, Iandiev I, Grosche J, Wiedemann P, Albrecht J, Reichenbach A: Role of retinal glial cells in neurotransmitter uptake and metabolism. Neurochem Int 2009;54:143-160.
52 Russo R, Rotiroti D, Tassorelli C, Nucci C, Bagetta G, Bucci MG, Corasaniti MT, Morrone LA: Identification of novel pharmacological targets to minimize excitotoxic retinal damage. Int Rev Neurobiol 2009;85:407-423.
53 Yamashita K, Kotani Y, Nakajima Y, Shimazawa M, Yoshimura S, Nakashima S, Iwama T, Hara H: Fasudil, a Rho kinase (ROCK) inhibitor, protects against ischemic neuronal damage in vitro and in vivo by acting directly on neurons. Brain Res 2007;1154:215-224.
54 Jeon S, Kim S, Park JB, Suh PG, Kim YS, Bae CD, Park J: RhoA and Rho kinase-dependent phosphorylation of moesin at Thr-558 in hippocampal neuronal cells by glutamate. J Biol Chem 2002;277:16576-16584.
55 Lewis G, Mervin K, Valter K, Maslim J, Kappel PJ, Stone J, Fisher S: Limiting the proliferation and reactivity of retinal Müller cells during experimental retinal detachment: the value of oxygen supplementation. Am J Ophthalmol 1999;128:165-172.
56 Kosako H, Amano M, Yanagida M, Tanabe K, Nishi Y, Kaibuchi K, Inagaki M: Phosphorylation of glial fibrillary acidic protein at the same sites by cleavage furrow kinase and Rho-associated kinase. J Biol Chem 1997;272:10333-10336.
57 Tramontina F, Leite MC, Cereser K, de Souza DF, Tramontina AC, Nardin P, Andreazza AC, Gottfried C, Kapczinski F, Gonçalves CA: Immunoassay for glial fibrillary acidic protein: antigen recognition is affected by its phosphorylation state. J Neurosci Methods 2007;162:282-286.
58 Ghiardi GJ, Gidday JM, Roth S: The purine nucleoside adenosine in retinal ischemia-reperfusion injury. Vision Res 1999;39:2519-2535.
59 Job C, Lagnado L: Calcium and protein kinase C regulate the actin cytoskeleton in the synaptic terminal of retinal bipolar cells. J Cell Biol 1998;143:1661-1672.
60 Shin T, Kim S, Ahn M, Kim H: An immunohistochemical study of protein kinase C in the bovine retina. J Vet Med Sci 2006;68:71-74.
61 Behrens UD, Borde J, Mack AF, Wagner HJ: Distribution of phosphorylated protein kinase C alpha in goldfish retinal bipolar synaptic terminals: control by state of adaptation and pharmacological treatment. Cell Tissue Res 2007;327:209-220.
62 Mueller BK, Mack H, Teusch N: Rho kinase, a promising drug target for neurological disorders. Nat Rev Drug Discov 2005;4:387-398
63 Salceda R, van Roosmalen GR, Jansen PA, Bonting SL, Daemen FJ: Nucleotide content of isolated bovine rod outer segments. Vision Res 1982;22:1469-1474.
64 Oberhoff P, Hockwin O: The ATP content of the retina in relation to the blood circulation. Albrecht von Graefes Arch Klin Exp Ophthalmol 1969;178:329-332.
65 Winkler BS: Glycolytic and oxidative metabolism in relation to retinal function. J Gen Physiol 1981;77:667-692.
66 Kandabashi T, Shimokawa H, Miyata K, Kunihiro I, Eto Y, Morishige K, Matsumoto Y, Obara K, Nakayama K, Takahashi S, Takeshita A: Evidence for protein kinase C-mediated activation of Rho-kinase in a porcine model of coronary artery spasm. Arterioscler Thromb Vasc Biol 2003;23:2209-2214.
67 Kaur C, Foulds WS, Ling EA: Hypoxia-ischemia and retinal ganglion cell damage. Clin Ophthalmol 2008;2:879-889.

Graefes Arch Clin Exp Ophthalmol
DOI 10.1007/s00417-014-2761-9

BASIC SCIENCE

Testing the effects of the dye Acid violet-17 on retinal function for an intraocular application in vitreo-retinal surgery

Aysegül Tura · Aizhan Alt · Christos Haritoglou · Carsten H. Meyer · Toni Schneider · Salvatore Grisanti · Julia Lüke · Matthias Lüke · for the International Chromovitrectomy Collaboration

Received: 30 April 2014 / Revised: 21 July 2014 / Accepted: 24 July 2014

Abstract
Purpose To facilitate epiretinal or inner limiting membrane peeling, dyes like Indocyanine Green (ICG) as well as Trypan Blue (TB) were used so far. However, toxic effects on the retina were described for both dyes. The aim of our study was to investigate the effects of a novel vital dye Acid violet-17 (AV-17) on retinal histology and function to assess a possible application in vitreo-retinal surgery.
Methods AV-17 was dissolved in a solvent with heavy water. An electroretinogram was recorded on perfused bovine retina. After reaching stable b-wave amplitudes, AV-17 (0.125–0.5 mg/ml) or the solvent was applied epiretinally for 30–300 seconds. The b-wave amplitudes were recorded before, during, and after treatment. Cultures of bovine retina were incubated for 30 or 300 seconds with the dye or solvent and processed for live/dead staining, immunohistochemistry, and immunoblotting.
Results Reductions of the b-wave amplitudes were observed directly after the exposure to AV-17, which were rapidly and completely reversible within the recovery period for all exposure times at the concentrations of 0.125 and 0.25 mg/ml as opposed to the partial recovery after exposure to 0.5 mg/ml. A high degree of damage in the ganglion cell layer (GCL) and glial reactivity were detected at the concentrations of 0.25 and 0.5 mg/ml but not after exposure to lower concentrations or the solvent.
Conclusion Application of AV-17 at a concentration of up to 0.125 mg/ml was well tolerated in terms of retinal function, survival in the GCL, and glial reactivity whereas higher concentrations are not recommended.

Keywords Acid violet-17 · Electroretinogram · Glial reactivity · Heavy water · Retinal biocompatibility · Vital dye · Vitreoretinal surgery

Introduction

Vital dyes have been used for more than ten years for macular surgery, allowing for an easier removal of the less recognizable structures like epiretinal membranes or the internal limiting membrane (ILM), which consist of a very lucent and thin tissue. Presently, trityl dyes such as brilliant blue G (BBG, Brilliant Peel) and patent blue V (PBV, Blueron) are available for chromovitrectomy. Both dyes have the best retinal biocompatibility compared to the other commonly used dyes such as indocyanine green (ICG) and trypan blue (TB), which have a higher potency to induce retinal toxicity [1–4]. BBG exhibits well-balanced characteristics regarding its staining qualities for the ILM and its retinal biocompatibility [5–7], though the concentrations higher than 0.25 mg/ml were not recommended due to the risk of toxicity [8]. A further limitation regarding the use of BBG arises from the inability to stain the epiretinal membranes sufficiently, rendering the use of its more toxic alternative TB as the "Gold Standard" for staining the epiretinal membranes. Similarly, patent blue V (PBV,

Aysegül Tura and Aizhan Alt contributed equally as first authors
Julia Lüke and Matthias Lüke contributed equally as senior authors

A. Tura · A. Alt · S. Grisanti · J. Lüke · M. Lüke (✉)
University Eye Hospital, University of Lübeck, Ratzeburger Allee 160, D-23538 Lübeck, Germany
e-mail: dr.matthias.lueke@googlemail.com

C. Haritoglou
Department of Ophthalmology, Ludwig Maximilian University, Munich, Germany

C. H. Meyer
Department of Ophthalmology, Aarau, Switzerland

T. Schneider
Institute of Neurophysiology, University of Cologne, Robert-Koch-Str. 39, D-50931 Köln, Germany

Published online: 14 September 2014

Blueron) is not of use in macular hole surgery due to its unfavourable staining qualities.

Currently, an alternative dye for TB is lacking. A new development to fill this need could be Acid violet-17 (AV-17/Coomassie violet R200), which is, similar to BBG, a novel trityl dye [9]. To improve the staining qualities, AV-17 should be applied with a special solvent carrier loaded with heavier water (D_2O), which leads to a higher density. This approach has already been tested to facilitate the sedimentation of BBG, for which a commercially available preparation in a solvent carrier loaded with heavy water currently exists (Brilliant Peel®, Fluoron GMBH, Ulm, Germany). The testing of this heavier formulation of the BBG dye showed no signs of toxicity in the model of the isolated bovine retina and in clinical use during vitreoretinal procedures in humans showing a tendency towards a slightly improved contrast between the ILM and the underlying retina [10–12].

In this study, we, therefore, investigated the retinal biocompatibility of the novel dye AV-17 dissolved in a heavier solvent carrier containing D_2O. To measure the effects of the exposure to this dye or its solvent alone for different time points on retinal function, we employed the electrophysiological ex-vivo technique of the isolated super fused bovine retina model, which is a very sensitive tool for testing retinal toxicity. [13] Moreover, we incubated the ganglion cell layer of cultured bovine retinas with the dye or its solvent to determine the extent of toxicity in this layer, which comprises the first group of retinal cells that come into direct contact with the dye after intraocular application. The reactivity of the astrocytes, Müller cells, and microglia were also evaluated after the exposure of the retinal cultures to the solvent or the different concentrations of the dye to gain insight into the magnitude of the retinal stress induced by these treatments.

Materials and methods

Chemicals and reagents

The analysis grade chemicals were purchased from Merck (Darmstadt, Germany). Acid violet-17 and the solvent carrier (composed of 0.13 ml D_2O in 1 ml H_2O with 1.9 mg Na_2HPO_4, 0.3 mg NaH_2PO_4, 8.2 mg NaCl) have been provided by Fluoron GMBH (Neu-Ulm, Germany). The culture medium (Neurobasal-A) and supplements (B-27, penicillin/streptomycin, L-Glutamine) were purchased from GIBCO (Invitrogen, Darmstadt, Germany). The brain-derived neurotrophic factor (BDNF) and ciliary neurotrophic factor (CNTF) were obtained from ReliaTech (Wolfenbüttel, Germany) and Invitrogen, respectively. Culture grade sterile phosphate buffered saline (PBS; without calcium and magnesium) and Hank's balanced salt solution (HBSS; with calcium and magnesium) were purchased from GIBCO. The cell culture grade bovine serum albumin (BSA) was obtained from Sigma-Aldrich (Munich, Germany). The antibodies and the fluorescent reagents used were as follows: mouse anti-CD11b (Serotec, Düsseldorf, Germany), rabbit anti-GFAP (DAKO, Hamburg, Germany), Cy3-conjugated goat anti-rabbit IgG (Jackson Immuno research, Dianova, Hamburg, Germany), Alexa 488-conjugated anti-mouse IgG (Molecular Probes, Invitrogen, Darmstadt, Germany), and horseradish peroxidase-conjugated secondary anti-rabbit or anti-mouse antibodies (Jackson Immuno research). The protease and phosphatase inhibitor cocktails were purchased from Roche Applied Sciences (Mannheim, Germany). All the remaining chemicals were obtained from Sigma-Aldrich.

Preparation of the AV-17 dye solution

The Acid Violet-17 dye was dissolved in the solvent supplied at the final concentrations between 0.00625 to 0.05 % (w/v, corresponding to a range between 0.0625–0.5 mg/ml) on a magnetic stirrer for 2–3 hours under light protection. The dye solution was sterile-filtered using 0.22 μm syringe filters, aliquotted at 1.5 ml, and stored at 4 °C until use. The aliquots were used within six months after preparation.

The isolated superfused vertebrate retina assay

Bovine eyes were obtained from a local slaughterhouse and harvested immediately postmortem. They were transported in darkness in a serum-free standard medium containing 120 mM NaCl, 2 mM KCl, 0.1 mM $MgCl_2$, 0.15 mM $CaCl_2$, 1.5 mM NaH_2PO_4, 13.5 mM Na_2HPO_4, and 5 mM glucose. Preparations were performed as described previously [6].

Each ERG was recorded in the surrounding nutrient medium via two silver/silver-chloride electrodes on either side of the retina. The recording chamber, containing a piece of retina, was placed in an electrically and optically insulated box. Perfusion velocity was controlled by a roller pump and set to 1 ml/min.

Temperature was kept constant at 30 °C. The perfusing medium was pre-equilibrated and saturated with oxygen and could be monitored by a Clark oxygen electrode. Retinas were dark-adapted, and ERGs were elicited at 5-min intervals using a single white flash for stimulation. The flash intensity was set to 6.3 mlx at the retinal surface using calibrated neutral density filters. The duration of light stimulation (500 ms) was controlled by a timer. ERGs were filtered and amplified (100-Hz high-pass filter, 50-Hz notch filter, 100.000× amplification) using a Grass CP 511 amplifier. Data were processed and converted using an analog-to-digital data acquisition board (NI USB-6221; National Instruments, Austin, TX, USA) and a personal computer. The ERGs were recorded and analysed by DASYLab Professional Version 10.0.0 (National Instruments, Austin, TX, USA).

Retinas were super fused with serum-free nutrient solution and stimulated repeatedly until stable b-wave amplitudes were recorded. Thereafter, the dye dissolved in solvent carrier at different concentrations or the solvent carrier alone, which were allowed to prewarm to room temperature for two hours, was applied epiretinally. The duration of retinal exposure was varied between 30 seconds and five minutes (30, 60, 120 and 300 seconds). After application of the dye solution (0.125, 0.25, or 0.5 mg/ml) the retina was reperfused with standard solution for at least 130 minutes. The b-wave amplitude was measured from the trough of the a-wave to the peak of the b-wave.

Treatment of retinal cultures with AV-17

Bovine eyes were obtained from a local slaughterhouse and harvested within two hours postmortem. The eyes were submerged for five minutes in an 11 % iodine solution (Betaisodona, Mundipharma GH, Limburg, Germany) under a laminar flow hood followed by rinsing twice with PBS for five minutes each. The eyes were dissected circumferentially 5 mm posterior to the limbus and the anterior segment and vitreous were removed. A 60 mm-piece of cellulose nitrate filter (0.45 μm pore size, Sartorius, Göttingen, Germany) was placed into a new 100 mm-Petri dish prefilled with fresh HBBS supplemented with calcium and magnesium. The retina was gently dissociated from the underlying pigment epithelium and transferred on to the cellulose nitrate filter in the Petri dish with the ganglion cell layer exposed. Pieces of retina with the underlying cellulose nitrate filter were dissected using a 6-mm biopsy punch along a radius of approximately 1 cm from the central retina. The retinal pieces and the underlying filter were transferred on to culture inserts with a pore size of 0.4 μm placed into a 6-well plate (n=2 retinas/insert). The wells were prefilled with 1 ml of culture medium (Neurobasal-A supplemented with 1X B-27, 1 % BSA, 1 mM L-Glutamine, 100 Units/ml penicillin, 100 μg/ml streptomycin, 50 ng/ml BDNF, 20 ng/ml CNTF, denoted as N+). A few drops of culture medium were also pipetted into the inserts at a volume barely sufficient to cover the retinas. The retinas were allowed to recover overnight in a 37 °C incubator with 5 % CO_2 and humidity.

On the following day, a new 6-well plate was prepared by filling the wells with 1 ml of fresh culture medium and placing new inserts of 0.4 μm pore size into each well. The retinas were placed on to the new inserts. The test substances (AV-17 at a concentration range of 0.0625–0.5 mg/ml; solvent; culture medium) were carefully pipetted into the inserts at a volume of 500 μl/insert, avoiding the detachment of the retinas from the filter underneath and ensuring that the ganglion cell layer was covered by the test substance. Retinas were incubated in duplicates with the test substances for 30 seconds or five minutes. Afterwards, the retinas were washed three times for five minutes with sterile PBS and placed back on to the initial culture inserts. The culture medium in each well of the initial culture plate was replenished 1:1 (v/v) with fresh medium and the retinas were incubated overnight at 37 °C as described above to allow for recovery.

Live/dead assay

Cultured retinas were transferred gently into the wells of a 24-well plate prefilled with PBS (n=1 retina piece/well), avoiding damage to the retinas. After rinsing briefly with PBS twice, retinas were incubated for 30 minutes in 4 μM Ethidium homodimer-1 (EthD-1) and 2 μM Calcein-AM (Molecular Probes) diluted in 0.1 % glucose-PBS. Afterwards, retinas were rinsed briefly with 0.1 % glucose-PBS twice and fixed with 2 % paraformaldehyde (PFA)-PBS for 15 minutes followed by 4 % PFA-PBS for 15 minutes. After three rinses in PBS for five minutes, the retinas were permeabilized in 0.1 % Triton X-100/PBS for ten minutes and counterstained with DAPI (1 μg/ml in PBS) for ten minutes to detect the nuclei. The retinae were rinsed twice in PBS, mounted in Mowiol, and analyzed by fluorescence microscopy (Leica, Wetzlar, Germany). To determine the percentage of damaged cells in each image, the number of EthD-1 positive (damaged) cells and the total cell number in that field (determined after the visualisation of the nuclei with DAPI) was quantified. Quantification of the stained cells was performed in 9–11 areas of 0.04 mm^2 per retina using the ImageJ software (NIH). Each experiment was performed using n=2 retinas per test group, for which the mean values were calculated. Data are presented as the mean ± standard error of mean (SEM) of n=3 independent experiments.

Immunohistochemistry on paraffin sections

Cultured retinas were fixed in formalin, embedded in paraffin, sectioned at 6 μm on a Leica RM2125RT microtome (Leica) and mounted on Fisherbrand SuperFrost Plus glass slides (Fisher Scientific, Houston, TX). After deparaffinization in Xylol for three times for five minutes and rehydration in a graded series of ethanol descending from 100 to 50 %, the slides were rinsed with PBS and blocked with PBS containing 3 % BSA and 0.3 % Triton X-100 (BSA-PBST) for 30 minutes at room temperature. The sections were incubated with the primary antibodies diluted in the blocking buffer overnight at 4 °C. Negative controls were incubated in the blocking buffer alone. The sections were rinsed in PBS and incubated with the fluorescent-secondary antibodies. The nuclei were counterstained with DAPI (1 μg/ml in PBS) for five minutes and the slides mounted with Mowiol were analyzed by fluorescence microscopy (Leica).

Immunohistochemistry on flat mounted retinas

For the immunohistochemical detection of glial reactivity in the nerve fiber layer of whole mounted retinas, the protocol of Wang et al., was performed with slight modifications [14]. Briefly, the whole mounted retinae were fixed in paraformaldehyde as above and washed three times for one hour in PBS containing 0.2 % Triton X-100. After blocking in 3 % BSA-PBST overnight at 4 °C, the retinas were incubated with the antibodies against CD11b (diluted 1/5 in the blocking buffer) or GFAP (1/200 in blocking buffer) for 48 hours at 4 °C to label the microglia or astrocytes/end-feet of Müller cells, respectively. The negative controls were incubated with the blocking buffer alone. Retinas were washed in PBS three times for one hour each and incubated with the secondary antibodies indicated above overnight at 4 °C. The nuclei were counterstained with DAPI for ten minutes and the retinae were analyzed by fluorescence microscopy. The quantification of the (CD11b)-positive cells was performed in four to five areas of 0.64 mm^2 on the flat mounted retinae using the ImageJ software.

Quantification of microglia reactivity

The morphological quantification of microglia in the nerve fiber layer of flat-mounted retinas was performed by calculating two different form factors as described [15, 16]. Briefly, the form factor 1 (FF1) is derived from the following equation:

$$\mathrm{FF1}: \frac{4\pi\, x \text{ cell area}}{(\text{cell perimeter})^2}$$

The FF1 ratio varies between 0 and 1, acquiring the latter value for a perfectly circular (ameboid) cell and decreasing as the number and/or length of the ramifications; hence, the cell perimeter increases. The FF1 serves as a sensitive indicator of initial ramification, since it decreases in the presence of even very short cytoplasmic processes. However, it does not always reflect the true degree of microglia reactivity, since an oval shaped cell without ramifications can also get a considerably lower FF1 value compared to the round, reactive microglia. For this purpose, we additionally quantified the microglia reactivity in terms of the FF2, which was calculated from the following ratio:

$$\mathrm{FF2}: \frac{\text{cell area}}{\text{convex area}}$$

The convex area is the area of a polygonal object demarcated by the cell's most extended projections. The FF2 ratio would approach 1 for an ameboid (reactive) cell, since both the normal and the convex areas would have similar values. In contrast, the long ramifications would significantly increase the convex area, resulting in the reduction of the FF2 ratio. The FF2 values thereby allow for a more specific grading of the presence of true, long ramifications. Quantification of the microglia area, perimeter, and the convex area was performed individually on each cell that was entirely localized within the boundaries of an image (n=5–8 images of 0.04 mm^2 per retina) using the Image J software. The FF1 and FF2 ratios were calculated individually for each cell and denoted as percentage. For each retina, the mean ± standard deviation (SD) of the FF1 and FF2 values were determined. The experiments were performed n=3 independent times. Quantifications presented here were performed on the retinas of a representative experiment.

Data analysis

The maximal percentage reduction of the b-wave amplitudes during application of AV-17 or the solvent carrier was expressed as the mean ± SD of n=3 experiments. The recovery of the b-wave was compared with the a-wave and b-wave amplitude before application of AV-17. For the statistical analysis the software "Origin 6.0" (Microcal) was used. Significance was estimated by the Student's t-test and levels of $p \leq 0.05$ were considered as statistically significant.

Results

The effects of AV-17 on retinal function in the isolated superfused vertebrate retina

Stable ERG-amplitudes were reached after a two-hour perfusion of the retinal preparations. Environmental parameters such as pH, osmotic pressure, temperature, and pO_2 of the perfusion medium remained unchanged during all conditions tested.

The b-wave amplitude is very sensitive for detecting retinal toxicity. At first we tested the solvent carrier including the heavy water at different exposure times (30, 60, 120 and 300 seconds) on the b-wave amplitude at the concentration of 0.13 ml/ml. We found a maximum b-wave reduction of 17.48±5.375 % directly after the application of the solvent carrier, which was not significant (p=0.07916). The maximum reduction of the b-wave amplitudes detected after longer exposure times (60 and 120 seconds) was less pronounced (7.74±6.1 and 3.88±3.84 %, respectively) and not significant (p=0.37721 and p=0.86621, respectively). For all tested exposure times, the ERG-amplitudes remained unimpaired throughout the washout and showed the same level compared to the amplitudes before application (p=0.32736 for 30 seconds; p=0.8542 for 60 seconds; p=0.24731 for 120 seconds). A similar observation could be made for the longest exposure time of 300 seconds. For both directly after the exposure (p=

0.23968) and at the end of the washout (p=0.92955), the solvent carrier did not induce a significant effect on the b-wave amplitude (Fig. 1).

The dye AV-17 was initially tested at a concentration of 0.25 mg/ml and led to a direct reduction of the b-wave amplitude after application, which was most prominent after the exposure time of 30 seconds (42.428±14.851 %; p=0.00115) and 120 seconds (41.498±13.64 %; p=0.0495). The exposure times of 60 and 300 seconds also led to a reduction of the b-wave amplitudes (37.55±12.71 and 31.19 ±10.57 %), which did not reach the level of significance (p=0.09744 and p=0.0845, respectively). A total abolishing of the b-wave briefly after the application of AV-17 was not observed in any of the test series. A full recovery of the b-wave amplitude was reached on an average of 20–25 minutes after applying AV-17 (Fig. 2).

At the end of the washout, the effects of the dye on the b-wave amplitudes remained fully reversible and the ERG-amplitudes returned to normal, showing no significant difference between the ERG-amplitudes before application for all the tested exposure times (p=0.12861 for 30 seconds; p=0.74135 for 60 seconds; p=0.28918 for 120 seconds; and p=0.078 for 300 seconds; Fig. 2).

As the next step, we tested AV-17 at a higher concentration of 0.5 mg/ml. The application for 30 seconds induced a significant reduction of 49.485±17.1827 % in the b-wave amplitude (p=0.04238). The effects on the b-wave amplitude were partially reversible at the end of the washout (41.745± 9.24189 %), but the impairment of full recovery did not reach the level of significance (p=0.07292). A longer exposure to the dye at the same concentration led to a stronger effect briefly after application. For an exposure time of 120 seconds, we found a significant reduction of 72.62±14.67954 % (p=

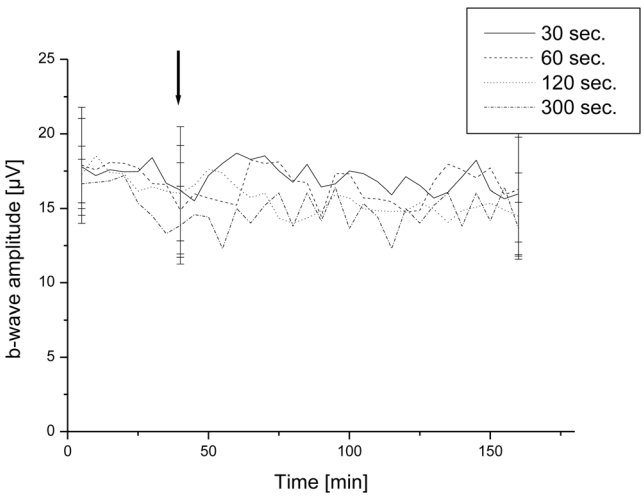

Fig. 1 Effects of the solvent carrier on the b-wave amplitude of the isolated perfused bovine retina. Average of representative test series. The *black arrow* marks the application of solvent carrier. Only the retinal exposure time was varied as indicated in the panel. A representative standard deviation for the test series is given

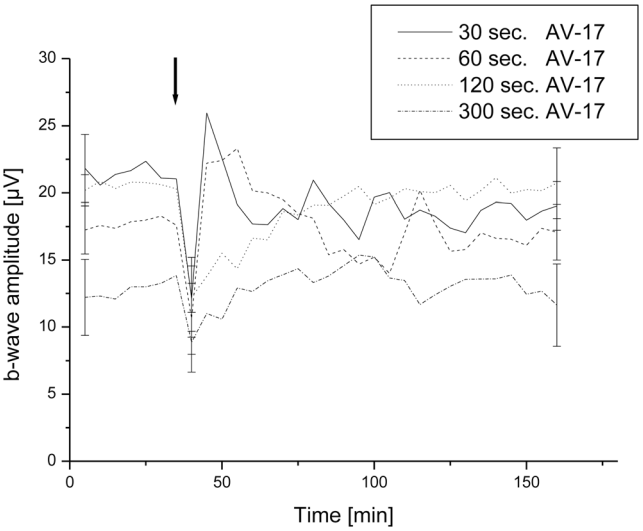

Fig. 2 Effects of 0.25 mg/ml AV-17 on the b-wave amplitude of the isolated perfused bovine retina. Average of representative test series. The *black arrow* marks the application of 0.25 mg/ml AV-17. Only the retinal exposure time was varied as indicated in the panel. A representative standard deviation for the test series is given

0.02801). The strongest effect could be observed after the application for five minutes, in which an average reduction of 78.265±7.48826 % (p=0.01922) could be recorded. The effects remained at least partially reversible at the washout, but for both exposure times the deficiency of recovery was not significant compared to the b-wave amplitudes before application (p=0.47203 ftwor 2 minutes and p=0.88266 for five minutes; Fig. 3).

We also tested a lower concentration of 0.125 mg/ml by applying the dye for 5 min and recorded an unsignificant reduction of 43.41±12.19052 % of the b-wave amplitude (p=0.12943). A fast recovery of the b-wave amplitude could be observed, and we detected that the effects were fully reversible at the end of the washout (p=0.88266).

Extent of cell viability in the ganglion cell layer after application of AV −17 or the solvent carrier

To determine the outcomes of the exposure to the dye or its solvent on the viability of the cells in the ganglion cell layer, cultured retinas were incubated with AV-17 (at a concentration range of 0.0625–0.5 mg/ml) or the solvent alone for 30 seconds or five minutes in duplicates. Retinas exposed to the fresh culture medium for 30 seconds or five minutes and washed similarly as the other treated retinas were included as controls. All the retinas were allowed to recover overnight in replenished culture medium after repeated washing. Extent of viability in the ganglion cell layer was determined by performing Live/Dead staining, which employs the usage of the fluorescent dyes Calcein-AM and Ethidium homodimer-1 (EthD-1). The former dye is a cell-permeable molecule which can be converted into a green fluorescent product by the

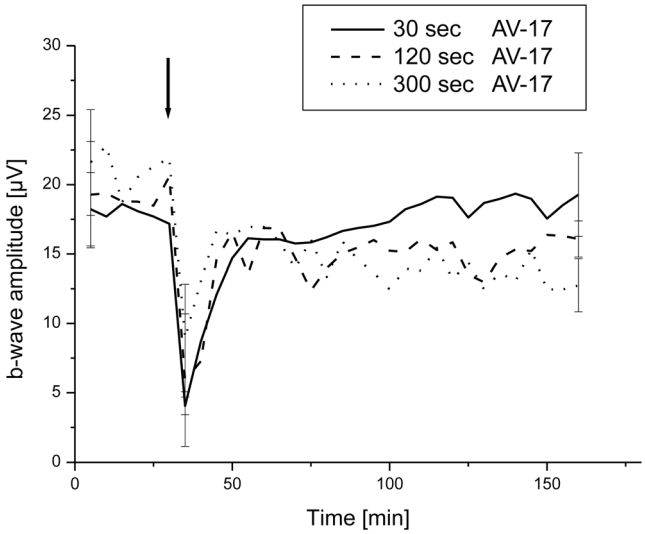

Fig. 3 Effects of 0.5 mg/ml AV-17 on the b-wave amplitude of the isolated perfused bovine retina. Average of representative test series. The *black arrow* marks the application of 0.5 mg/ml AV-17. Only the retinal exposure time was varied as indicated in the panel. A representative standard deviation for the test series is given

esterases in living cells. In contrast, EthD-1 is a membrane–impermeable red fluorescent dye, which can only enter the cells with damaged membranes.

The control retinas treated with the culture medium alone exhibited a high degree of viability as demonstrated by the strong Calcein-AM staining and the very low level of EthD-1 uptake, which was restricted to only 9.69 +/− 6.06 % of the cells in the ganglion cell layer after five minutes of treatment (mean ± SEM of $n=3$ experiments). Retinas treated with the solvent alone also exhibited a high level of viability with very low levels of EthD-1 uptake (13.26±7.76 % after 5 minutes of exposure, $p=0.5168$ compared to the retinas treated with medium). Exposure of the retinas to the dye at the concentrations of 0.0625 and 0.125 mg/ml did not result in a decrease in the levels of Calcein-AM, though the EthD-1 staining became gradually stronger as the concentration of the dye and the exposure time increased (20.88±3.99 % with 0.0625 mg/ml dye and 20.56± 9.71 % with 0.125 mg/ml dye after five minutes; $p=$ 0.1809 and $p=0.3482$, respectively, compared to the solvent alone; Figs. 4 and 5).

With increasing concentrations (0.25 and 0.5 mg/ml) of the dye, we observed a decline in the Calcein-AM staining and an increase in the uptake of EthD-1 particularly after the 5-minute exposure (36.29±5.94 and 36.63±9.47 %, respectively), which was significant compared to the retinas treated with the solvent alone ($p=0.0029$ and $p=$ 0.0163, respectively; Figs. 4 and 5), demonstrating a considerable decrease in viability after the exposure to the dye at higher concentrations.

Extent of astrocyte and Müller cell activation in response to AV-17 or the solvent carrier

The extent of astrocyte reactivity in the nerve fiber layer was initially analysed after a 5-minute exposure of the cultured retinas to the solvent or AV-17 at an intermediate concentration of 0.125 mg/ml and at the highest tested concentration of 0.5 mg/ml in duplicates. Retinas exposed to the fresh culture medium alone for five minutes and washed similarly to the other treated retinas were included as controls. All the retinas were allowed to recover overnight in culture medium after repeated washing. The control retinas treated with the culture medium alone exhibited a modest immunoreactivity for GFAP on the nerve fiber layer, suggesting that the astrocytes are in a quiescent state. The retinas treated with the solvent alone also exhibited a very low degree of GFAP-immunoreactivity, suggesting that the solvent did not activate the astrocytes after a 5-minute exposure and was thereby well tolerated by the retina (Fig. 6a).

A slight increase in GFAP expression and fiber thickness was observed after the application of the dye at an intermediate concentration of 0.125 mg/ml (Fig. 6a). The macroscopic evaluation of the retinas also revealed that the dye was weakly retained on the nerve fiber layer despite the repeated washing steps and the overnight recovery in culture medium (data not shown). Exposure to AV-17 at a concentration of 0.5 mg/ml resulted in a remarkable upregulation in the GFAP levels as opposed to all the other groups, suggesting that the application led to a considerable degree of retinal stress (Fig. 6a). The dye was also retained at considerably higher levels in the nerve fiber layer and was readily discernible by macroscopic evaluation (data not shown).

Similarly, the immunostainings for GFAP on the retinal cross sections demonstrated a quiescent state of not only the astrocytes in the nerve fiber layer, but also the Müller cells in the retinas treated with the culture medium or solvent alone for both 30 seconds and five minutes. A slight upregulation of GFAP was observed in the nerve fiber layer and Müller cells in response to a 5-minute exposure to the dye treatment at the concentrations of 0.0625 and 0.125 mg/ml compared to the retinas treated with the solvent carrier. With increasing concentrations of the dye (0.25 and 0.5 mg/ml), the upregulation of GFAP became more prominent in both the Müller cells and the nerve fiber layer even after an exposure of 30 seconds, demonstrating a gradual increase in the reactivity of astrocytes and Müller cells in response to higher concentrations of the dye (Fig. 6b).

Extent of microglia reactivity in response to AV-17 or the solvent carrier

Microglial reactivity was quantified based on two form factors (FF) that provide a numerical score (0-100 %) for cellular

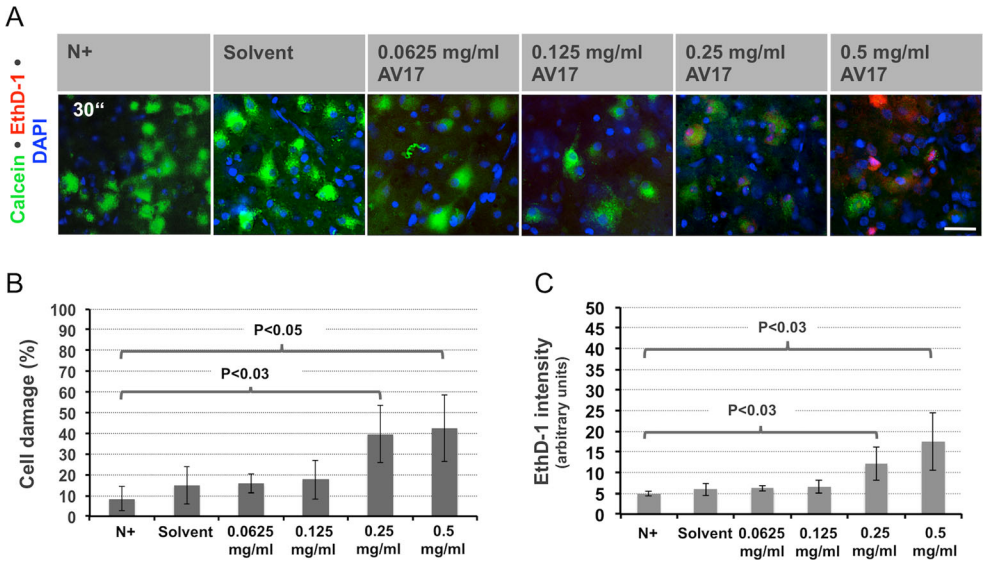

Fig. 4 Viability of the cells in the ganglion cell layer after exposure to AV-17 or its solvent for 30 seconds. (**a**) Representative images of the live/dead staining demonstrating a gradual decrease in the processing of the vital dye Calcein (*green*) and an increase in the uptake of the membrane-impermeable dye Ethidium homodimer-1 (EthD-1, *red*) in the ganglion cell layer of the retinas exposed to 0.25 and 0.5 mg/ml AV-17 for 30 seconds. Retinas incubated with the normal culture medium (N+) were included as the baseline controls. *Bar*=10 μm. (**b**) Quantification of the percentage of damaged (EthD-1 positive) cells in the ganglion layer. Data represent the mean ± SEM obtained of n=3 experiments for 0.0625 and 0.5 mg/ml, and n=4 experiments for the remaining groups. (**c**) Quantification of the intensity of EthD-1 uptake in the ganglion cell layer. Data represent the mean ± SEM obtained of n=3 experiments for 0.0625 and 0.5 mg/ml, and n=4 experiments for the remaining groups

morphology, acquiring lower values for the quiescent, ramified cells and approaching 100 % as the microglia transformed into a more ameboid, reactive morphology with a decrease in the number and/or length of the protrusions. The FF1 value decreases with the presence of even very short protrusions whereas the FF2 value is a more sensitive indicator of true

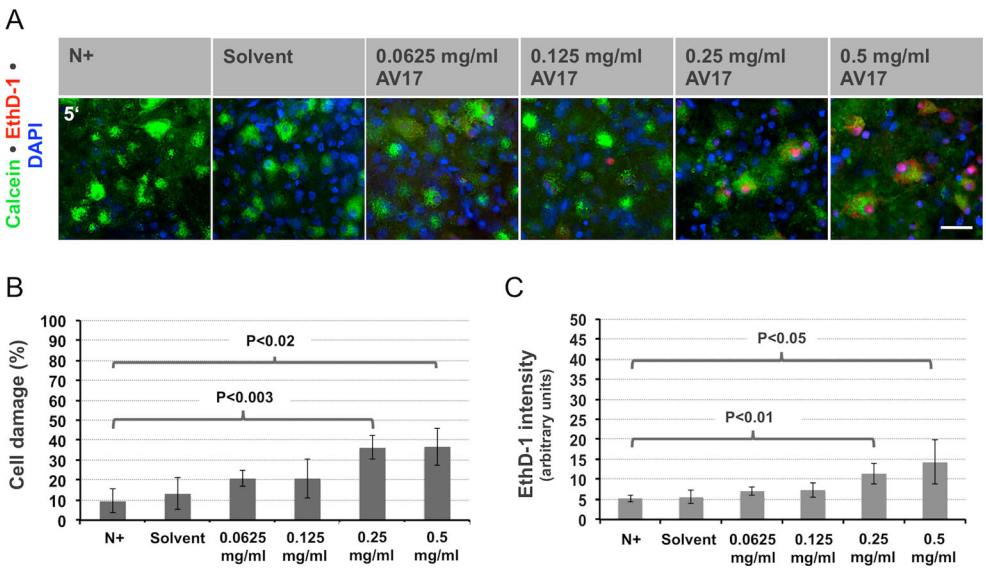

Fig. 5 Viability of the cells in the ganglion cell layer after exposure to AV-17 or its solvent for five minutes. (**a**) Representative images of the live/dead staining on the ganglion cell layer. Exposure to the AV-17 dye at the higher concentrations of 0.25 and 0.5 mg/ml for five minutes resulted in a considerable increase in the percentage of damaged cells with the uptake of the membrane-impermeable dye Ethidium homodimer-1 (EthD-1, *red*). Retinas incubated with the normal culture medium (N+) were included as the baseline controls. *Bar*=10 μm. (**b**) Quantification of the percentage of damaged (EthD-1 positive) cells in the ganglion cell layer. Data represent the mean ± SEM obtained of n=3 experiments for 0.0625 n=5 experiments for the solvent, and n=4 experiments for the remaining groups. (**c**) Quantification of the intensity of EthD-1 uptake in the ganglion cell layer. Data represent the mean ± SEM obtained of n=3 experiments for 0.0625 n=5 experiments for the solvent, and n=4 experiments for the remaining groups

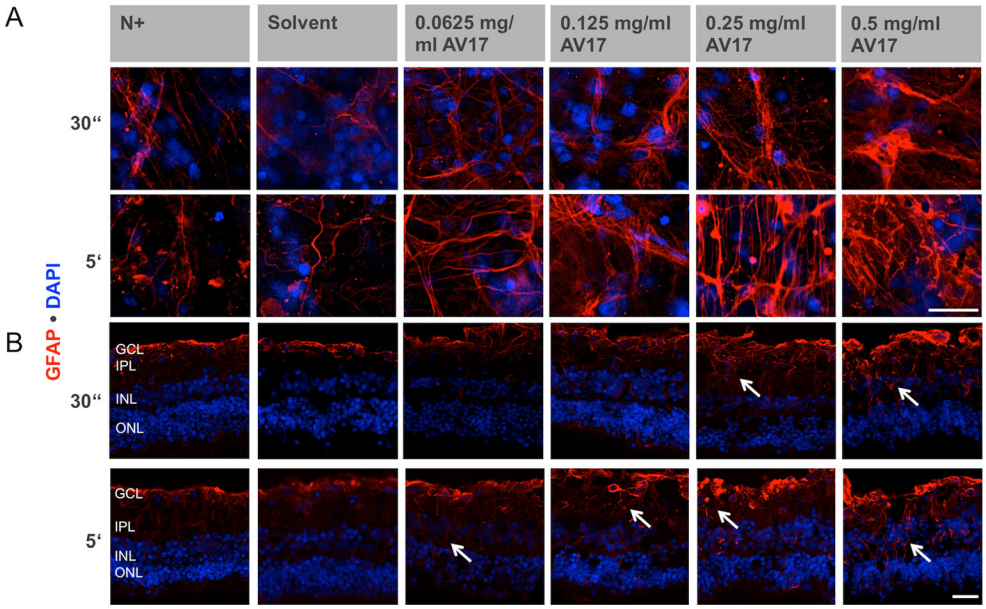

Fig. 6 Outcomes of the exposure to AV-17 or its solvent on the reactivity of astrocytes and Müller cells. Exposure of the ganglion cell layer (GCL) to AV-17 resulted in a time-dependent and dose-dependent increase in the reactivity of both (**a**) the astrocytes in the nerve fiber layer and (**b**) the Müller cells that extend radially, as demonstrated by the immunostainings for GFAP (*red*) on the flat mounts and transverse paraffin sections of the treated retinas, respectively. *Bar* indicates 50 and 25 μm in (**a**) and (**b**), respectively. Retinas incubated with the normal culture medium (N+) were included as the baseline controls. The nuclei were counterstained in *blue* with DAPI. IPL: Inner plexiform layer; INL: Inner nuclear layer; ONL: Outer nuclear layer

ramifications with long and branched protrusions. Microglia in the nerve fiber layer were visualised by performing immunostainings for the marker protein CD11b on the flat-mounted retinal cultures.

Microglia in the control retinas treated with the culture medium for five minutes exhibited the quiescent morphology with numerous long and branched protrusions (Fig. 7). This quiescent morphology was retained to a high extent in the retinas treated with the solvent alone for five minutes, which was also evident from the very low values for FF1 (3.16± 0.53 %; mean ± SD of n=14 images of 0.04 mm^2 from a representative experiment). The majority of the microglia in the retinas exposed to AV-17 at the concentrations of 0.125 and 0.5 mg/ml also exhibited a ramified morphology. However, the number and length of these protrusions were gradually reduced with increasing concentrations of the dye, as reflected by the FF1 score of 5.33±0.66 and FF2 score of 76.57±4.89 % detected for the group treated with 0.5 mg/ml AV-17 for five minutes (mean ± SD of n=14 images of 0.04 mm^2 from a representative experiment, $p<0.0001$ for both scores compared to the retina treated with the solvent alone; Fig. 7).

Discussion

The model of the isolated and perfused vertebrate bovine retina is a very sensitive and standardized tool for evaluating retinal toxicity of drugs [13]. Besides the functional analysis, our model allows for an intensive histological, ultrastructural, or biochemical evaluation of the tested retinae [17–19]. We tested the effects of AV-17 on the b-wave amplitude because the b-wave amplitude is the most sensitive criterion to detect changes reflecting the integrity of the inner neural network of the retina [10, 20]. Similar results could be demonstrated after dye application for bovine and human retina in which our experimental setup corresponds most closely to the situation in vivo where the dye is directly applied on the retinal surface [21]. However, the ERG reflects only the function of the photoreceptors and the activity of the network of the inner retina, whereas the function of the ganglion cell layer, which comprises the first group of retinal cells that would come into contact with the dye after intraocular application, could not be recorded. We, therefore, additionally performed cultures of flat-mounted bovine retina to evaluate the outcomes of the exposure to the dye or its solvent on the viability of the cells in the ganglion cell layer and the reactivity of glial cells.

At first we tested the solvent carrier alone, which includes deuterium oxide (heavy water; D_2O) to enhance the staining effects of the dye. Deuterium (symbol: D) is a stable isotope of hydrogen, and was discovered in 1932 by Harold Urey [22]. It has been shown that mammals can tolerate a concentration of up to 30 % of D_2O in drinking water, and that a short exposure to a blood serum deuterium fraction of up to 0.23 ml/ml appeared safe [23, 24]. In our experimental setup, we detected no significant effects on the b-wave amplitude directly after

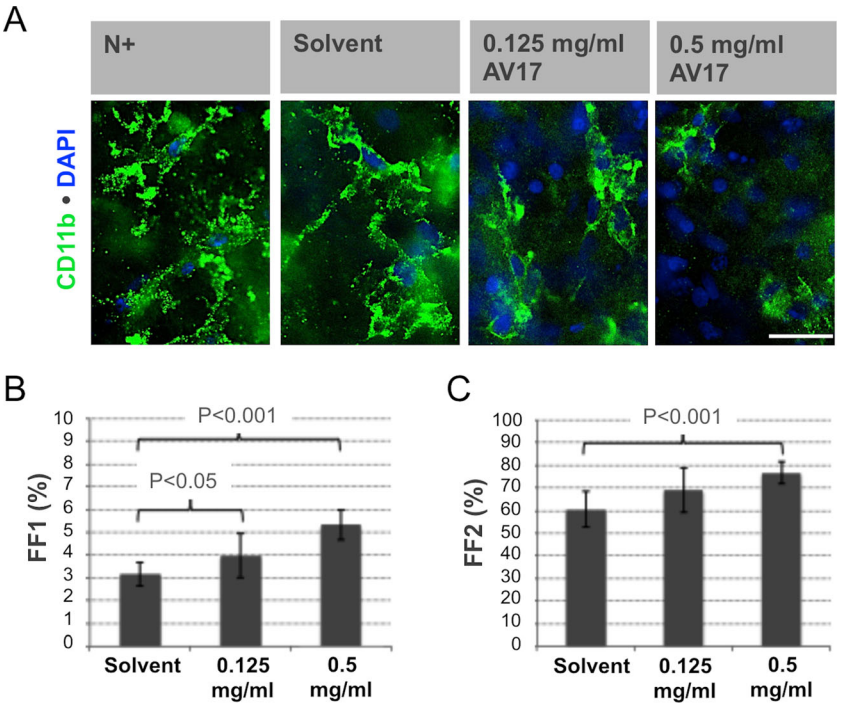

Fig. 7 Outcomes of the exposure to AV-17 or its solvent on the reactivity of microglia. Microglia in the nerve fiber layer of flat-mounted retinas exposed to the solvent alone or 0.125 mg/ml AV17 exhibited a quiescent morphology characterized by the long and branched ramifications as detected by the CD11b immunostaining (*green*). In contrast, a considerable decrease was observed in the number and length of the protrusions of the microglia in the retinas exposed to 0.5 mg/ml AV-17, demonstrating the transition into a more reactive phenotype. The nuclei were counterstained in *blue* with DAPI. Retinas incubated with the normal culture medium (N+) were included as the baseline controls. The images are representative of $n=3$ independent experiments. *Bar*=50 μm. Quantification of microglial reactivity was performed by determining the form factors (FF) 1 and 2 (**b**, **c**) from a representative experiment. Data represent the mean ± standard deviation of $n=6$–12 regions of 0.04 mm^2

the application of the solvent carrier (containing 0.13 ml D_2O/ml) or during the washout even after a long exposure time of five minutes. Additionally, the exposure of the retinal cultures to the solvent did not result in a considerable decrease in viability. The solvent carrier was very well tolerated not only in terms of cell survival in the ganglion cell layer but also the extent of glial reactivity, resulting in no considerable activation of the astrocytes, Müller cells or the microglia compared to the normal retinas treated with medium. These results are in accordance with recently reported investigations of a solvent carrier for BBG including the same concentration of D_2O in an isolated retinal preparation [10].

A reduction of the ERG amplitudes of the isolated perfused vertebrate retina was noticed after the application of AV-17 for all test series. However, the measured decrease in the ERG-amplitudes could not be solely interpreted as a toxic effect. In fact, the reduction of the ERG amplitudes can be explained by the absorption of the applied light via the dye, since the dye was applied between the retina and the source of light. Therefore, the applied light would be initially absorbed by the dye before reaching the retina, resulting in a decrease in the intensity of the stimulus. This view was further supported by the kinetics of the ERG-amplitudes, demonstrating that the recovery occurred simultaneously with the complete disappearance of the dye from the perfusion chamber. Moreover, a recovery was observed after application for all test series (0.125-0.5 mg/ml) independent from the retinal exposure time and used concentration, showing no significant prolonged effects on the b-wave amplitude at the washout. Application of AV-17 in combination with a D_2O containing solvent was, therefore, regarded as safe for the normal functioning of the photoreceptors and the inner retinal network.

Exposure to the dye at the concentrations of 0.0625 mg/ml and 0.125 mg/ml was also well tolerated by the retinal cells in terms of the cellular viability in the ganglion cell layer and the maintenance of glial cells in a quiescent state. However, we found some remarkable effects on cell viability at the higher concentrations of 0.25 mg/ml and 0.5 mg/ml, with a significant increase in cell damage in the ganglion cell layer already after an exposure of 30 seconds, which became more prominent after prolonged treatment. This was associated with the activation of astrocytes and Müller cells, providing further evidence of the ongoing retinal stress. Exposure of the cultured retinas to the solvent alone or the dye at a concentration of 0.125 μg/ml did not result in a noticeable increase in microglia reactivity, suggesting that the tissue stress did not reach a critical level that would necessitate a macrophagic cleaning process. However, the treatment with 0.5 mg/ml of the dye also led to a significant increase in the number of microglia acquiring a more reactive phenotype.

A possible reason underlying these concentration dependent effects on the cultured retinas might be the residues of the dye retained in the nerve fiber layer even after extensive washing steps and the overnight recovery in replenished culture medium. Being responsible for maintaining homeostasis in the retina, the glial cells would react to the presence of any foreign substance and be involved in the management of the new environmental conditions [25–27]. The reactivity of the astrocytes and Müller cells to even the low concentrations of AV-17 that remained after the exposure to the dye at 0.0625–0.125 mg/ml was, therefore, possibly a homeostatic response. Though the glial reactivity is initially attempted as a protective response, an excessive reactivity of these cells can also have adverse effects on the adjacent neurons [25–27]. The extent of viability in the ganglion cell layer was indeed reduced after the long-term exposure to the dye at high concentrations together with an increase in glial reactivity. Yet, we should also consider that the lack of a perfusion system in our culture model might also have accounted for the retaining of the dye in the nerve fiber layer, whereas in an in vivo system with a normal vasculature, the dye is not expected to accumulate at such high concentrations and be gradually cleared. Application of AV-17 at higher concentrations is, therefore, likely to be well tolerated in vivo without such adverse effects. Nevertheless, we consider it safer to apply the dye at a concentration of 0.125 mg/ml or lower to avoid excessive glial reactivity and adverse effects on retinal cell viability.

Our findings are also mainly in accordance with the results of a previously published study investigating the retinal biocompatibility of AV-17, which was reported to be superior to the biocompatibility of trypan blue and indocyanine green. However, contrary to our findings, a good biocompatibility was stated even for the concentration of 0.5 mg/ml [9]. In the former study, the dye was applied intravitreally into the vitreous humor. The discrepancy to our study might, therefore, have resulted from the protective effects of the vitreous humor, which was described in detail for the drug triamcinolone. [28–30]. Moreover, the intravitreal injection into the vitreous would also result in the dilution of the dye solution in the vitreous before reaching the nerve fiber layer and thereby a more gradual exposure of the retinal cells to the dye solution as opposed to the direct application of the dye on to the nerve fiber layer in our electrophysiological and retinal culture models.

AV-17 belongs to the same group of substances, the trityl dyes, like BBG and PBV. Both dyes have been investigated in our model of the isolated perfused retina. Comparing our results of AV-17 with our former experiences with BBG and PBV, the effects AV-17 on the ERG were very similar to BBG, and we think that both dyes have the same biocompatibility. [6] However, the best biocompatibility is with PB, but this dye has only low staining capabilities. [4] Therefore, the staining of the ILM with AV-17 at the suggested concentrations could be applicable. A recent study indeed demonstrated that a 3-minute exposure of vitrectomized cadaveric eyes to 0.05 mg/ml of an acid violet dye enabled the distinction of ILM from the underlying retina with a high degree of contrast and facilitated the surgical peeling of ILM [31]. However, the optimal concentration required to stain the epiretinal membranes remains to be determined, since a staining of epiretinal membranes with BBG was not observed at a concentration of 0.25 mg/ml [5]. If the staining of epiretinal membranes can be satisfactorily achieved with AV-17, the usage of this dye would lead to a substantial progress in vitreo-macular surgery by representing an alternative for the more toxic dye trypan blue. Otherwise AV-17 can be appreciated as an alternative to BBG for ILM-staining like newly developed formulations of BBG [32].

Based on our results, we conclude that the application of AV-17 at a concentration of 0.125 mg/ml or below in a D_2O-carrying solvent appears safe for intraocular administration. Nevertheless, similar to the intraocular application of BBG, restricting the time the retina is exposed to this novel dye would be advisable to avoid adverse effects through excessive glial reactivity. The in vivo staining characteristics and acceptance of a new formulation of AV-17/D_2O in clinical practice also need to be established.

Acknowledgments We would like to thank Ms. Christine Örün for her technical assistance with the preparation of paraffin sections. This study was supported by the Federal Ministry of Economics and Technology on the basis of a decision of the German Bundestag: KF2335702UL9.

Conflict of interest None.

References

1. Cheng SN, Yang TC, Ho JD, Hwang JF, Cheng CK (2005) Ocular toxicity of intravitreal indocyanine green. J Ocul Pharmacol Ther 21: 85–93
2. Haritoglou C, Gandorfer A, Gass CA, Schaumberger M, Ulbig MW, Kampik A (2002) Indocyanine green-assisted peeling of the internal limiting membrane in macular hole surgery affects visual outcome: a clinicopathologic correlation. Am J Ophthalmol 134:836–841
3. Kanda S, Uemura A, Yamashita T, Kita H, Yamakiri K, Sakamoto T (2004) Visual field defects after intravitreous administration of indocyanine green in macular hole surgery. Arch Ophthalmol 122:1447–1451
4. Lüke C, Lüke M, Dietlein TS, Hueber A, Jordan J, Sickel W, Kirchhof B (2005) Retinal tolerance to dyes. Br J Ophthalmol 89(9):1188–91
5. Enaida H, Hisatomi T, Hata Y, Ueno A, Goto Y, Yamada T, Kubota T, Ishibashi T (2006) Brilliant blue G selectively stains the internal limiting membrane/brilliant blue G-assisted membrane peeling. Retina 26:631–636
6. Lüke M, Januschowski K, Beutel J, Lüke C, Grisanti S, Peters S, Jaissle GB, Bartz-Schmidt KU, Szurman P (2008) Electrophysiological effects of brilliant blue G in the model of the isolated perfused vertebrate retina. Graefes Arch Clin Exp Ophthalmol 246:817–822

7. Enaida H, Kumano Y, Ueno A, Yoshida S, Nakao S, Numa S, Matsui T, Ishibashi T (2013) Quantitative analysis of vitreous and plasma concentrations of brilliant blue g after use as a surgical adjuvant in chromovitrectomy. Retina 33(10):2170–4
8. Enaida H, Hisatomi T, Goto Y, Hata Y, Ueno A, Miura M, Kubota T, Ishibashi T (2006) Preclinical investigation of internal limiting membrane staining and peeling using intravitreal brilliant blue G. Retina 26:623–630
9. Cardoso EB, Moraes-Filho M, Rodrigues EB, Maia M, Penha FM, Novais EA, Souza-Lima RA, Meyer CH, Farah ME (2013) Investigation of the retinal biocompatibility of acid violet for chromovitrectomy. Graefes Arch Clin Exp Ophthalmol 251(4): 1115–21
10. Januschowski K, Mueller S, Spitzer MS, Schramm C, Doycheva D, Bartz-Schmidt KU, Szurman P (2012) Evaluating retinal toxicity of a new heavy intraocular dye, using a model of perfused and isolated retinal cultures of bovine and human origin. Graefes Arch Clin Exp Ophthalmol 250:1013–1022
11. Haritoglou C, Schumann RG, Kampik A, Gandorfer A (2011) Heavy brilliant blue G for internal limiting membrane staining. Retina 31(2): 405–407
12. Henrich PB, Valmaggia C, Lang C, Priglinger SG, Haritoglou C, Strauss RW, Cattin PC (2013) Contrast recognizability during brilliant blue G - and heavier-than-water brilliant blue G-assisted chromovitrectomy: a quantitative analysis. Acta Ophthalmol 91(2): e120–124
13. Lüke M, Weiergräber M, Brand C, Siapich SA, Banat M, Hescheler J, Lüke C, Schneider T (2005) The isolated perfused bovine retina - a sensitive tool for pharmacological research on retinal function. Brain Res Brain Res Protoc 16:27–36
14. Wang L, Cioffi GA, Cull G, Dong J, Fortune B (2002) Immunohistologic evidence for retinal glial cell changes in human glaucoma. Invest Ophthalmol Vis Sci 43(4):1088–94
15. Heppner FL, Roth K, Nitsch R, Hailer NP (1998) Vitamin E induces ramification and downregulation of adhesion molecules in cultured microglial cells. Glia 22:180–188
16. Alt A, Hilgers RD, Tura A, Nassar K, Schneider T, Hueber A, Januschowski K, Grisanti S, Lüke J, Lüke M (2013) The neuroprotective potential of Rho-kinase inhibition in promoting cell survival and reducing reactive gliosis in response to hypoxia in isolated bovine retina. Cell Physiol Biochem 32(1):218–34
17. Sickel W (1972) Electrical and metabolic manifestations of receptor and higher-order neuron activity in vertebrate retina. Adv Exp Med Biol 24:101–118
18. Sickel W (1972) Retinal metabolism in dark and light. In: Autrum H, Jung R, Loewenstein WR, MacKay DM, Teuber HL (eds), Handbook of Sensory Physiology. Springer-Verlag, 667–727
19. Lüke M, Januschowski K, Beutel J, Warga M, Grisanti S, Peters S, Schneider T, Lüke C, Bartz-Schmidt KU, Szurman P (2008) The effects of triamcinolone crystals on retinal function in a model of isolated perfused vertebrate retina. Exp Eye Res 87:22–29
20. Block F, Schwarz M (1998) The b-wave of the electroretinogram as an index of retinal ischemia. Gen Pharmacol 30:281–287
21. Lüke C, Lüke M, Sickel W, Schneider T (2006) Effects of patent blue on human retinal function. Graefes Arch Clin Exp Ophthalmol 244: 1188–1190
22. Bradley CA, Urey H (1932) The relative abundance of hydrogen isotopes in natural hydrogen. Phys Rev 40:889–890
23. Medina DC, Li X, Springer CS Jr (2005) Pharmaco-thermodynamics of deuterium-induced oedema in living rat brain via 1H2O MRI: implications for boron neutron capture therapy of malignant brain tumours. Phys Med Biol 50:2127–2139
24. Thomson JF (1960) Physiological effects of D_2O in mammals. Ann N Y Acad Sci 84:736–744
25. Bringmann A, Pannicke T, Grosche J, Francke M, Wiedemann P, Skatchkov SN, Osborne NN, Reichenbach A (2006) Müller cells in the healthy and diseased retina. Prog Retin Eye Res 25(4):397–424
26. Langmann T (2007) Microglia activation in retinal degeneration. J Leukoc Biol 81(6):1345–51
27. Johnson EC, Morrison JC (2009) Friend or foe? Resolving the impact of glial responses in glaucoma. J Glaucoma 18(5):341–53
28. Szurman P, Kaczmarek R, Spitzer MS, Jaissle GB, Decker P, Grisanti S, Henke-Fahle S, Aisenbrey S, Bartz-Schmidt KU (2006) Differential toxic effect of dissolved TA and its crystalline crystals on cultured human retinal pigment epithelium (ARPE19) cells. Exp Eye Res 83:584–592
29. Szurman P, Sierra A, Kaczmarek R, Jaissle GB, Wallenfels-Thilo B, Grisanti S, Lüke M, Bartz-Schmidt KU, Spitzer MS (2007) Different biocompatibility of crystalline TA crystals on retinal cells in vitro and in vivo. Exp Eye Res 85:44–53
30. Spitzer MS, Mlynczak T, Schultheiss M, Rinker K, Yoeruek E, Petermeier K, Januschowski K, Szurman P (2011) Preservative-free triamcinolone acetonide injectable suspension versus "traditional" triamcinolone preparations: impact of aggregate size on retinal biocompatibility. Retina 31(10):2050–7
31. Penha FM, Pons M, Costa EF, Barros NM, Rodrigues EB, Cardoso EB, Dib E, Maia M, Marin-Castaño ME, Farah ME (2013) Retinal pigmented epithelial cells cytotoxicity and apoptosis through activation of the mitochondrial intrinsic pathway: role of indocyanine green, brilliant blue and implications for chromovitrectomy. PLoS One 8(5):e64094
32. Maia M, Furlani BA, Souza-Lima AA, Martins DS, Navarro RM, Belfort R Jr (2014) LUTEIN: a new dye for chromovitrectomy. Retina 34(2):262–72

Original Paper

Ophthalmic Research

Ophthalmic Res 2014;51:167–171
DOI: 10.1159/000357284

Received: October 1, 2013
Accepted: November 13, 2013
Published online: March 13, 2014

The Concentration-Dependent Effects of Indocyanine Green on Retinal Function in the Electrophysiological ex vivo Model of Isolated Perfused Vertebrate Retina

Mahdy Ranjbar[a] Aizhan Alt[a] Khaled Nassar[a] Mihaela Reinsberg[a]
Toni Schneider[b] Salvatore Grisanti[a] Julia Lüke[a] Matthias Lüke[a]

[a]University Eye Hospital, University of Lübeck, Lübeck, and [b]Institute of Neurophysiology, University of Cologne, Cologne, Germany

Key Words
Electroretinogram · Indocyanine green · Ocular dyes · Macular surgery

Abstract
Background: Dye solutions such as indocyanine green (ICG) are used for the staining of intraocular structures. The aim of the presented study was to investigate the effects of ICG on bovine retinal function using different concentrations of ICG. ***Methods:*** Bovine retina preparations were perfused with a standard solution and the electroretinogram was recorded. The nutrient solution was substituted by an ICG solution at varying concentrations for 45 min. Afterwards the preparations were reperfused with standard solution for at least 85 min. ***Results:*** Significant reductions in b-wave amplitude were found for concentrations of 0.0025% ($p = 0.0099$) and 0.025% ($p = 0.0378$). For the concentration of 0.025%, the b-wave amplitude remained significantly decreased ($p = 0.0082$) after the observation period, but a full recovery of the b-wave was observed for the concentration of 0.0025% ($p = 0.1917$). ***Conclusion:*** Intraocular application of sufficient ICG concentrations for internal limiting membrane staining seems not possible without interfering with retinal function.

Introduction

Clinical use of intraocular dyes for staining the internal limiting membrane (ILM) and epiretinal membranes leads to improvement in anatomical success and functional outcome after vitreomacular surgery [1, 2]. The first dye applied for this indication was indocyanine green (ICG), which has been used in internal medicine for over half a century [3]. After intraocular use of ICG without specific toxicological testing on the retina, concerns soon arose, and morphological and functional changes after its application have been reported [4, 5]. Therefore, alternatives with better retinal biocompatibility, such as Brilliant Blue G, were investigated and in part replaced ICG [6]. Nevertheless, today ICG is still frequently used in vitreomacular surgery.

Several experimental studies have used cell cultures to investigate the toxicity of ICG to the retina [7, 8]. It was demonstrated that high concentrations of ICG caused more reduction in retinal pigment epithelium cell viability [9]. But using these in vitro models has the disadvan-

J.L. and M.L. contributed equally to this study and should be regarded as equivalent senior authors.

KARGER

E-Mail karger@karger.com
www.karger.com/ore

0030–3747/14/0513–0167$39.50/0

PD Dr. med. M. Lüke
University Eye Hospital, University of Lübeck
Ratzeburger Allee 160
DE–23538 Lübeck (Germany)
E-Mail matthias.lueke@uk-sh.de

tage of being unable to reproduce the functional retinal impact in vivo. However, we have previously shown that the isolated superfused bovine retina is an adequate, sensitive model for pharmacological testing [10]. Using this model, we were able to demonstrate the time-dependent toxic impact of ICG on retinal function [11].

Therefore, the purpose of this study was to examine the impact of different ICG concentrations on retinal function in the isolated superfused bovine retina model, which proved to be closer to actual in vivo findings and displayed lower susceptibility to interfering in vivo parameters than observed in study animals [10, 12]. Effects were analyzed based on the parameters of the electroretinogram (ERG). Our aim was to define a safe concentration of ICG which simultaneously allows a sufficient staining of the ILM for macular surgery.

Materials and Methods

Materials

Glucose and the constituents of the nutrient solution (analytical grade) used for superfusion of the bovine retina were purchased from Merck (Darmstadt, Germany). All stock solutions for the nutrient solutions were sealed in glass tubes (Gerresheimer Wertheim GmbH, Wertheim, Germany) to establish reproducibility of ERG recordings. Deionized water (<0.1 μS/cm) was additionally glass distilled and autoclaved in glass bottles. All solutions were prepared in autoclaved glass bottles, using sterile distilled water.

Superfused Vertebrate Retina Assay

Freshly enucleated bovine eyes were opened equatorially, the vitreous was removed and circular pieces of the posterior segment were obtained using a 7-mm trephine. The retina was separated from the underlying pigment epithelium and mounted on a mesh occupying the center of a perfusion chamber.

An ERG was recorded in the surrounding nutrient via 2 silver/silver chloride electrodes on either side of the retina. The chamber was installed in an electrically and optically isolated air thermostat. Perfusion velocity was controlled by a roller pump (1 ml/min) and the temperature was kept constant at 30°C. The perfusion medium was preequilibrated with oxygen and the oxygen level monitored by a Clarke electrode. The ERG was elicited at intervals of 5 min using a single white flash (6.3 mlx, 500 ms) controlled by a timer-operated mechanical shutter system. The ERG was amplified and bandpass limited between 0.1 and 300 Hz. The signal was AD converted and stored using a PC-based signal acquisition and analyzing system. The retina was perfused with serum-free standard medium (NaCl 120, KCl 2, $MgCl_2$ 0.1, $CaCl_2$ 0.15, Na_2HPO_4 13.5 and glucose 5 mmol/l) and stimulated repeatedly until stable amplitudes were reached.

Then, 50 mg of ICG (Pulsion Medical Systems, Munich, Germany) were dissolved in 10 ml of sterile distilled water, and 1 ml of the resulting solution was diluted each with varying volumes of BSS Plus (Alcon Surgical, Fort Worth, Tex., USA), forming the different final concentrations of 0.000025, 0.00025 and 0.05%. For the ICG solutions with a concentration of 0.0025 and 0.025%, ICG was directly dissolved in the nutrient solution to avoid a shift of the well-balanced nutrient solution.

For each concentration (0.025, 0.0025, 0.00025 and 0.000025%) a new isolated retina was used (n = 3–4). The retina was superfused with the serum-free nutrient solution and stimulated repeatedly until stable amplitudes were recorded. The standard medium was replaced by one of these ICG concentrations for 45 min (retinal exposure time). Afterwards, the preparation was reperfused with standard medium for at least 85 min.

To show the validity of the recently published data on dye biocompatibility, we performed one additional test series using the concentration of 0.05%. After recording stable b-wave amplitudes, the 0.05% ICG solution was applied for 21 s. Following this, the retina was reperfused with standard solution for at least 115 min (n = 5).

Data Analysis

The b-wave amplitude was measured from the trough of the a-wave to the peak of the b-wave, and the percentage of b-wave reduction after exposition was calculated. Changes in b-wave amplitude were carefully monitored. Furthermore, reversibility of the impact of ICG on the b-wave after reperfusion with standard medium was considered. For statistical analysis of the b-wave amplitude, the software Origin 6.0 (MicroCal) was used. Significance was calculated with Student's t test. Levels of $p \leq 0.05$ were regarded as statistically significant, and $p \leq 0.01$ as highly significant.

Results

Stable ERG amplitudes were reached within 2 h of perfusion of the retinal preparations. The environmental parameters for the perfusion medium, such as pH, osmotic pressure, temperature and P_{O_2} remained unchanged during substitution with the dye solution.

The exposure of ICG at a concentration of 0.05% for 21 s led to a highly significant reduction in b-wave amplitude ($p = 0.00161$) by abolishing the responses directly after exposure (fig. 1). However, after reperfusion with standard nutrient solution, the b-wave amplitude recuperated, and at the end of the washout a partial recovery was observed in which the b-wave amplitude was not significantly different to the amplitudes prior to exposure.

During exposure with lower-concentrated ICG solutions for 45 min, a significant reduction ($p < 0.05$) in b-wave amplitude was found for the concentrations of 0.025 and 0.0025%. The lowest tested concentrations (0.00025 and 0.000025%) did not have any statistically significant impact on the ERG during exposure (table 1; fig. 2). The reversibility of the dye effect proved to be concentration dependent as well. While the b-wave amplitude recovered during the 85 min after exposure with 0.0025% ICG solution (no significant persistent b-wave reduction; p =

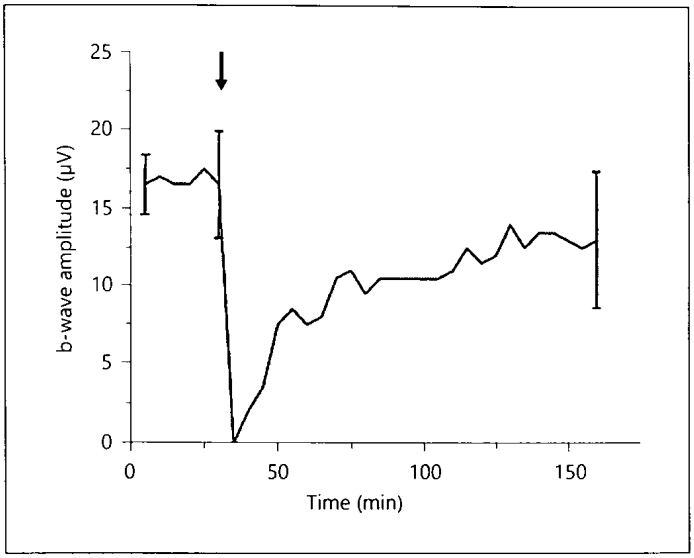

Fig. 1. Effects of ICG on b-wave amplitude of isolated perfused bovine retina. Average of representative drug series. Black arrow: application of 0.05% ICG for 21 s (n = 5). The representative standard deviation for the test series is given.

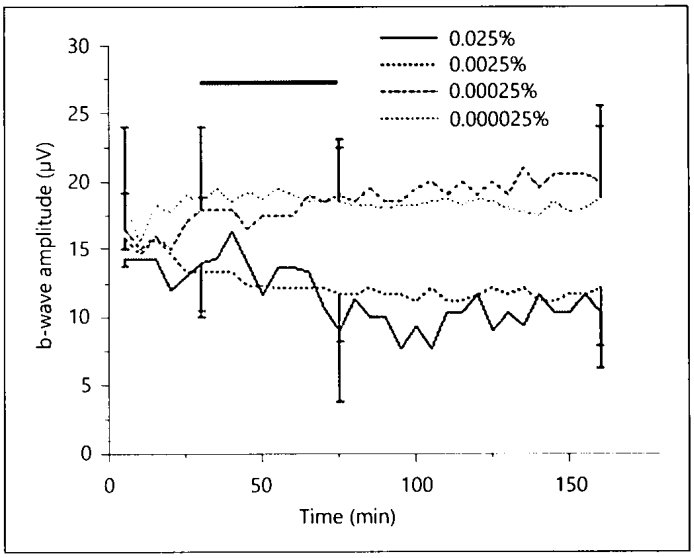

Fig. 2. Effects of ICG on b-wave amplitude of isolated perfused bovine retina. Average of representative drug series. Horizontal bar: application of indicated different concentrations for 45 min. The representative standard deviation for the test series is given.

Table 1. ERG results directly after ICG exposure

ICG concentration	PBR, %	p
0.025%	−38.9 (19.3)	0.0378*
0.0025%	−13.4 (5.8)	0.0099**
0.00025%	+3.7 (16.0)	0.9879
0.000025%	+5.6 (19.2)	0.6667

Values in parentheses denote standard deviations. * $p \leq 0.05$, ** $p \leq 0.01$. PBR = Persistent b-wave reduction.

Table 2. ERG results 85 min after ICG exposure and reperfusion with standard medium in the meantime

ICG concentration	PBR, %	p
0.025%	−27.7 (9.6)	0.0082**
0.0025%	−10.4 (10.0)	0.1917
0.00025%	+6.6 (28.5)	0.9142
0.000025%	+11.1 (25.9)	0.7509

Values in parentheses denote standard deviations. ** $p \leq 0.01$. PBR = Persistent b-wave reduction.

0.1917), it still remained decreased after the same time when a concentration of 0.025% was applied (significant persistent b-wave reduction; p = 0.0082). The lower concentrations tested did not lead to a significant deficiency in b-wave recovery during the washout (table 2; fig. 2).

Discussion

The purpose of this study was to evaluate the effects of different concentrations of ICG on retinal function. As many types of retinal cells and synapses are involved in the generation of the b-wave, it might be obvious that a reduction in this parameter indicates significant dysfunction of retinal neurons. Therefore, the b-wave amplitude is a very sensitive indicator of retinal dysfunction and is a useful tool for detecting drug biocompatibility.

There has been growing experimental and even clinical evidence that ICG might not be as safe as previously thought. Major visual-field defects have been reported after ICG-assisted ILM delamination, whereas there were none in patients who underwent conventional peeling without any dye [5, 13]. Furthermore, severe damage was described after experimental macular surgery and application of 0.05% ICG solution to human donor eyes, presuming that ICG induces a phototoxic effect on the vitreoretinal surface resulting in a disruption of Müller cells [4, 14, 15]. Actually, since then this photosensitivity-related impact of ICG has been effectively used to treat different kinds of cancer experimentally and even clinically

[16, 17]. Moreover, a cell culture study demonstrated a dose-related increase in expression of apoptotic genes after cells were exposed to 2.5 mg/ml (0.25%) ICG solution and light, while it was not observed in controls and with a concentration of 0.25 mg/ml (0.025%) [7].

Several animal studies on ICG have been performed. Most of them showed a concentration-dependent retinal impact associated with ICG. For instance, it has been demonstrated that the ERG and histology of rabbit eyes treated with 0.5 mg/ml (0.05%) ICG were normal 1 week after intravitreal injection, whereas higher concentrations of 5 mg/ml (0.5%) and 25 mg/ml (2.5%) ICG resulted in dark-adapted ERG abnormalities and histological examination revealed morphological changes [18, 19].

A clinical study evaluating changes in macular function and potential retinal toxicity in epiretinal membrane surgery with ICG-assisted ILM peeling using multifocal electroretinography showed no significant changes in N1 and P1 response amplitudes and peak latencies when a concentration of 0.5 mg/ml (0.05%) was used, whereas a concentration of 1.25 mg/ml (0.125%) resulted in significant amplitude reductions compared with baseline [20, 21].

Considering lower concentrations than 0.0025% of ICG might be a simple solution to avoid retinal toxicity, but these concentrations induce problems regarding sufficient visualization of the ILM. Kwok et al. [21] showed that a concentration of 1.25 mg/ml (0.125%) might be needed to achieve stable, excellent visualization of the ILM to grant safe removal during macular surgeries. Lower concentrations such as 0.5 mg/ml (0.05%) and 0.25 mg/ml (0.025%) achieved an at least adequate staining only in 77% (0.5 mg/ml) and 50% (0.25 mg/ml) of all cases [20]. Despite these facts, ICG is still used by some surgeons due to its favorable staining properties. The concentrations of the intraoperatively applied ICG solutions vary between 0.025% and 0.5% [2, 13, 15]. But, as our experiments have shown, even a concentration of 0.025% does have toxic short-term effects on retinal function in ERG.

Nevertheless, these results should be interpreted with caution. Despite the fact that this model mimics the intraoperative situation after fluid/air exchange properly, it remains an ex vivo model. In addition, the application time might have been exaggerated (45 min), since from a clinical point of view it is much shorter (1–5 min) [4, 5]. But being determined empirically, this duration of 45 min shows solid validity in regard to evaluating toxic effects on retinal functions, as demonstrated in previous studies [22, 23].

With regard to application time, we have already demonstrated that a concentration of 0.05% ICG leads to reversible effects on the ERG after retinal exposure of up to 30 s. Exceeding the exposure time of 30 s resulted in persistent impairment of retinal function [11]. These findings were confirmed during this study when a 0.05% ICG solution was applied for 21 s. Thus, toxic effects on retinal function after intraoperative short-term application of 0.05% ICG are unlikely to occur. However, it has been demonstrated that despite careful intraoperative removal of the dye, infrared fluorescence of ICG may persist up to 3 years after ICG-assisted vitrectomy and that, therefore, the actual application time leading to adverse effects might be much longer than expected [24].

In conclusion, our data from an isolated, superfused retina model indicate that besides exposure time there is also a concentration-dependent impact of ICG on retinal function. ICG solutions at a concentration of 0.025% or higher have persistent effects on retinal function. Lower concentrations might be safe, at least regarding the ERG, but are not clinically applicable on account of their decreasing staining ability. Therefore, the continuous use of ICG in macular surgery should be called into question, because a safe concentration with sufficient staining properties might not exist for ICG solutions.

Disclosure Statement

The authors state no conflict of interest.

References

1 Slaughter K, Lee IL: Macular hole surgery with and without indocyanine green assistance. Eye (Lond) 2004;18:376–378.

2 Kwok AKH, Lai TYY, Li WWY, Woo DCF, Chan NR: Indocyanine green-assisted internal limiting membrane removal in epiretinal membrane surgery: a clinical and histologic study. Am J Ophthalmol 2004;138:194–199.

3 Cherrick G, Stein S, Leevy C, Davidson C: Indocyanine green: observations on its physical properties, plasma decay, and hepatic extraction. J Clin Invest 1960;39:592–600.

4 Haritoglou C, Gandorfer A, Gass CA, Schaumberger M, Ulbig MW, Kampik A: Indocyanine green-assisted peeling of the internal limiting membrane in macular hole surgery affects visual outcome: a clinicopathologic correlation. Am J Ophthalmol 2002;134:836–841.

5 Kanda S, Uemura A, Yamashita T, Kita H, Yamakiri K, Sakamoto T: Visual field defects after intravitreous administration of indocyanine green in macular hole surgery. Arch Ophthalmol 2004;122:1447–1451.

6 Baba T, Hagiwara A, Sato E, Arai M, Oshitari T, Yamamoto S: Comparison of vitrectomy with Brilliant Blue G or indocyanine green on retinal microstructure and function of eyes with macular hole. Ophthalmology 2012;119:2609–2615.
7 Yam HF, Kwok AKH, Chan KP, Lai TYY, Chu KY, Lam DSC, Pang CP: Effect of indocyanine green and illumination on gene expression in human retinal pigment epithelial cells. Invest Ophthalmol Vis Sci 2003;44:370–377.
8 Ho JD, Tsai RJF, Chen SN, Chen HC: Cytotoxicity of indocyanine green on retinal pigment epithelium: implications for macular hole surgery. Arch Ophthalmol 2003;121:1423–1429.
9 Rezai KA, Farrokh-Siar L, Ernest JT, van Seventer GA: Indocyanine green induces apoptosis in human retinal pigment epithelial cells. Am J Ophthalmol 2004;137:931–933.
10 Lüke M, Weiergräber M, Brand C, Siapich SA, Banat M, Hescheler J, Lüke C, Schneider T: The isolated perfused bovine retina: a sensitive tool for pharmacological research on retinal function. Brain Res Brain Res Protoc 2005;16:27–36.
11 Lüke C, Lüke M, Dietlein TS, Hueber A, Jordan J, Sickel W, Kirchhof B: Retinal tolerance to dyes. Br J Ophthalmol 2005;89:1188–1191.
12 Bartz-Schmidt KU, Brunner R, Esser P, Lüke C, Walter P, Sickel W: The triple flash electroretinogram and its significance in macular diseases: b-wave recovery as a diagnostic tool. Graefes Arch Clin Exp Ophthalmol 1996;234:604–611.
13 von Jagow B, Höing A, Gandorfer A, Rudolph G, Kohnen T, Kampik A, Haritoglou C: Functional outcome of indocyanine green-assisted macular surgery: 7-year follow-up. Retina 2009;29:1249–1256.
14 Gandorfer A, Haritoglou C, Gandorfer A, Kampik A: Retinal damage from indocyanine green in experimental macular surgery. Invest Ophthalmol Vis Sci 2003;44:316–323.
15 Haritoglou C, Gandorfer A, Gass CA, Schaumberger M, Ulbig MW, Kampik A: The effect of indocyanine-green on functional outcome of macular pucker surgery. Am J Ophthalmol 2003;135:328–337.
16 Barth BM, Altinoğlu EI, Shanmugavelandy SS, Kaiser JM, Crespo-Gonzalez D, DiVittore NA, McGovern C, Goff TM, Keasey NR, Adair JH, Loughran TP Jr, Claxton DF, Kester M: Targeted indocyanine-green-loaded calcium phosphosilicate nanoparticles for in vivo photodynamic therapy of leukemia. ACS Nano 2011;5:5325–5337.
17 Li X, Naylor MF, Le H, Nordquist RE, Teague TK, Howard CA, Murray C, Chen WR: Clinical effects of in situ photoimmunotherapy on late-stage melanoma patients: a preliminary study. Cancer Biol Ther 2010;10:1081–1087.
18 Maia M, Kellner L, de Juan E Jr, Smith R, Farah ME, Margalit E, Lakhanpal RR, Grebe L, Au Eong KG, Humayun MS: Effects of indocyanine green injection on the retinal surface and into the subretinal space in rabbits. Retina 2004;24:80–91.
19 Penha FM, Maia M, Eid Farah M, Príncipe AH, Freymüller EH, Maia A, Magalhães O Jr, Smith RL: Effects of subretinal injections of indocyanine green, trypan blue, and glucose in rabbit eyes. Ophthalmology 2007;114:899–908.
20 Lai TYY, Kwok AKH, Au AWH, Lam DSC: Assessment of macular function by multifocal electroretinography following epiretinal membrane surgery with indocyanine green-assisted internal limiting membrane peeling. Graefes Arch Clin Exp Ophthalmol 2007;245:148–154.
21 Kwok AKH, Lai TYY, Yew DTW, Li WWY: Internal limiting membrane staining with various concentrations of indocyanine green dye under air in macular surgeries. Am J Ophthalmol 2003;136:223–230.
22 Lüke M, Januschowski K, Lüke J, Peters S, Wirtz N, Yörük E, Lüke C, Bartz-Schmidt KU, Grisanti S, Szurman P: The effects of ranibizumab (Lucentis) on retinal function in isolated perfused vertebrate retina. Br J Ophthalmol 2009;93:1396–1400.
23 Lüke M, Januschowski K, Tura A, Lüke J, Nassar K, Lüke C, Schneider T, Szurman P, Grisanti S, Bartz-Schmidt KU: Effects of pegaptanib sodium on retinal function in isolated perfused vertebrate retina. Curr Eye Res 2010;35:248–254.
24 Sekiryu T, Iida T: Long-term observation of fundus infrared fluorescence after indocyanine green-assisted vitrectomy. Retina 2007;27:190–197.